


6-2016

Sedimentology of Kingston Peak Formation KP1 Beds in Beck Canyon Region, Kingston Range, California

Dominic Joel Ombati

Follow this and additional works at: <http://scholarsrepository.llu.edu/etd>

 Part of the [Geology Commons](#), and the [Sedimentology Commons](#)

Recommended Citation

Ombati, Dominic Joel, "Sedimentology of Kingston Peak Formation KP1 Beds in Beck Canyon Region, Kingston Range, California" (2016). *Loma Linda University Electronic Theses, Dissertations & Projects*. 399.
<http://scholarsrepository.llu.edu/etd/399>

This Thesis is brought to you for free and open access by TheScholarsRepository@LLU: Digital Archive of Research, Scholarship & Creative Works. It has been accepted for inclusion in Loma Linda University Electronic Theses, Dissertations & Projects by an authorized administrator of TheScholarsRepository@LLU: Digital Archive of Research, Scholarship & Creative Works. For more information, please contact scholarsrepository@llu.edu.

LOMA LINDA UNIVERSITY
School of Medicine
in conjunction with the
Faculty of Graduate Studies

Sedimentology of Kingston Peak Formation KP₁ Beds in Beck Canyon
Region, Kingston Range, California

by

Dominic Joel Ombati

A thesis submitted in partial satisfaction of
the requirements for the degree
Master of Science in Geology

June 2016

© 2016

Dominic Ombati
All Rights Reserved

Each person whose signature appears below certifies that this thesis in his opinion is adequate, in scope and quality, as a thesis for the degree Master of Science.

_____, Chairperson
Kevin E. Nick, Associate Professor of Geology

Stanley Awramik, Professor of Geology

H. Paul Buchheim, Professor of Geology

ACKNOWLEDGEMENTS

I would like to express my gratitude to several people and institutions that contributed to the success of this research. Funds for the project were provided by the Faith and Science Council. The Loma Linda University Department of Earth and Biological Sciences supported me with a tuition waiver and living stipend that enabled me to complete this project.

I would like to appreciate clear guidance, willingness to help at all times and patience of my advisor Dr. Kevin Nick. The rest of my committee members Dr. Paul Buchheim and Dr. Stanley Awramik were vital in the revision and corrections of this manuscript and giving further guidance for this project.

I would also like to thank my neighbor Loren Libby and our lab technician Wayne Kelln for accompanying me to the field during my two independent field trips. And finally, I would like to thank my wife Rose and my one-year-old son Joshua for their love and support that keeps me going.

CONTENT

Approval Page.....	iii
Acknowledgements.....	iv
List of Figures	viii
List of Tables	ix
List of Abbreviations	x
Abstract.....	xi
Chapter	
1. Expanded introduction	1
Introduction.....	1
Stratigraphy.....	1
Beck Spring Dolomite.....	2
Kingston Peak Formation	3
KP ₁	4
KP ₂ , KP ₃ and KP ₄	5
Beck Spring Dolomite-Kingston Peak Formation boundary	5
Geological setting	6
Geochronology.....	6
Brief history of research.....	7
Snowball earth	8
Microbialites	9
Petrography of Kingston Peak subunits	10
KP ₁	10
KP ₂	11
KP ₃	11
KP ₄	11
References.....	12

2. Sedimentology Kingston Peak Formation KP ₁ Beds in Beck Canyon Region, Kingston Range, California	15
Abstract	15
Introduction.....	16
Geological setting	17
Stratigraphy.....	19
Beck Spring Dolomite.....	19
Kingston Peak Formation	19
Beck Spring Dolomite-Kingston Peak Formation boundary	20
Method	21
Results.....	22
General description of the outcrop	22
Facies	28
Facies 1: Altered dolomite/ karst	28
Facies 2: Interbedded dolostones and silty mudstones	32
Thinly interbedded silty dolostones and silty mudstones	32
Thinly interbedded sandy dolostones and silty mudstones.....	35
Facies 3: Bedded fine sand	35
Mineralogy.....	39
Sections	41
A and B beds.....	47
Bed thickness in facies 2.....	53
Discussion.....	54
Provenance	54
Provenance from quartz	55
Provenance from feldspars.....	56
Provenance from accessory minerals.....	58
Provenance from textural immaturity	59
Paleoenvironmental interpretation of facies	59
Facies 1: Altered dolostones	59
Facies 2: Interbedded dolostones and silty mudstones	60
Tide dominated delta.....	61

Tidal flats	62
Mixed carbonate-siliciclastic deposits	63
Facies 3: Bedded fine sandstones	64
Correlations	64
Beck Spring Dolomite-Kingston Peak Formation boundary	65
Conclusions	66
References	68
3. Expanded conclusions and future research	71
Appendices	
A. XRD data from Kingston Range locations	72
B. XRD data for A and B beds	74
C. SEM-EDS from Kingston Range locations	75
D. SEM-EDS data for A and B beds	76
E. A & B bed thickness data from Kingston Range locations	77

FIGURES

Figures	Page
1.1. Two major glaciations during Neoproterozoic time	9
2.1. Map showing the study area	18
2.2. Google Earth and topographic maps showing the study area	23
2.3. Field appearance at location 1.....	25
2.4. Field appearance at location 2.....	26
2.5. Field appearance at location 3.....	27
2.6. Photo of the field appearance of facies 1 in location 1	29
2.7. Photo showing wavy and crinkled microbial laminations	30
2.8. Photographs of facies 1 in thin section	31
2.9. Photographs of the field appearance of facies 2	33
2.10. Photographs facies 2 lithologies in thin section.....	34
2.11. Photographs of field appearance of facies 3	36
2.12. Photographs of facies 3 in thin section from location 1.....	37
2.13. Photo of a birefringent tourmaline grain.....	38
2.14. Section 1.....	43
2.15. Section 2.....	45
2.16. Section 3.....	46
2.17. Detailed section of the base of location 1	49
2.18. Detailed section of the base of location 2	51
2.19. Detailed section of the base of location 3	52
2.20. Thin beds average thickness trends.....	54

TABLES

Tables	Page
1.1. Comparative Stratigraphy of the Pahrump Group	3
2.1. List of location coordinates for the areas studied	22
2.2. XRD mineralogy from location 1	40
2.3. XRD mineralogy from location 2	40
2.4. XRD mineralogy from location 3	41
3.1. XRD data for location 1	72
3.2. XRD data for location 2	72
3.3. XRD data for location 3	73
3.4. XRD data for location 1 A and B thin beds	74
3.5. XRD data for location 2 A and B thin beds	74
3.6. XRD data for location 3 A and B thin beds	74
3.7. SEM-EDS data for location 1	75
3.8. SEM-EDS data for location 2	75
3.9. SEM-EDS data for location 3	75
3.10. SEM-EDS data for location 1 A and B thin beds	76
3.11. SEM-EDS data for location 2 A and B thin beds	76
3.12. SEM-EDS data for location 3 A and B thin beds	76
3.13. A and B bed thickness data for location 1	77
3.14. A and B bed thickness data for location 2	78
3.15. A and B bed thickness data for location 3	79

ABBREVIATIONS

BSD	Beck Spring Dolomite
EDS	Energy Dispersive Spectroscopy
KPF	Kingston Peak Formation
SEM	Scanning Electron Microscope
XRD	X-Ray Diffraction

ABSTRACT OF THE THESIS

Sedimentology of Kingston Peak Formation KP₁ Beds in Beck Canyon
Region, Kingston Range, California

by

Dominic Joel Ombati

Master of Science Graduate Program in Geology
Loma Linda University, June 2016
Dr. Kevin E. Nick, Chairperson

The Neoproterozoic Kingston Peak Formation (KPF) is known for its diamictites interpreted as of glacial origin. The KPF overlies the Beck Spring Dolomite (BSD) that contains microfossils and microbialites. This study aims to test correlation between outcrops and understand the abrupt change from BSD to KPF. It focuses on the basal 4 meters of the KP₁ subunit of the KPF as it appears in the Beck Canyon region, Kingston Range, California. We describe and correlate sedimentary rocks at and immediately overlying the contact and analyze the sedimentary structures, textures and sequences.

We have found only three sites in the northern Kingston Peak Range where the contact can be observed. At each site we measured sections about 4 meters long across the contact. The top of the BSD in all locations contains microbial laminations, oncoids, pisoids, sheets of chert and peloids. Thin sections from about 15 cm below the contact to about 50 cm above the contact show microbial laminations with some peloids or ghosts of peloids and abundant chert. The base of the KPF is composed of millimeter to centimeter-scale alternating two bed types named A-bed and B-bed. A-beds are clastic-rich and B-beds are dolomite-rich. A-beds are dolomitic silty mudstones with abundant muscovite. B-beds are recrystallized silty dolostones with peloid ghosts. A few of the

beds show faint current ripple cross bedding, cross bedding and lenticular structures. A to B bed contacts are sharp. At all stratigraphic levels, clastics have immature textures and compositions. XRD and thin section analysis show a trend of decreasing dolomite up-section. Measurement and analysis of individual alternating bed thickness show cyclical patterns and a gradational increase in bed thickness to massive sandstones.

Mineralogical patterns, pisoid-rich layers, and bed thickness patterns can all be correlated among the three sections. The pattern of increasing clastic content and bed thickness upsection suggests clastic influx during progradation that progressively overwhelmed carbonate production. This progradational setting could have occurred on a tide dominated delta or on a prograding tidal flat. The BSD-KPF contact at Kingston Range most likely represent a sequence boundary as evidenced by a change in lithology from dolostones to clastics.

CHAPTER ONE

EXPANDED INTRODUCTION

Introduction

The Neoproterozoic Kingston Peak Formation (KPF) is known for its diamictites thought to represent glacial processes (Mrofka, 2010; Petterson, 2009). Studies in the underlying Beck Spring Dolomite (BSD) describe microfossils and microbialites that suggest warm and shallow water (Gutstadt, 1968; Loyd and Corsetti, 2010). This study aims to understand an abrupt change from BSD to KPF as it appears in the Beck Canyon region, Kingston Range, California.

The objective of this study is to understand the depositional conditions in the environment recorded in the basal 4 meters of the KP₁ unit by establishing correlations and examining depositional processes in the Kingston Range area. The basal KPF is a significantly different depositional setting than BSD. Chapter one reviews some literature related to this study specifically on stratigraphy, Beck Spring Dolomite - Kingston Peak Formation boundary, geological setting, geochronology, a brief history of research in the Pahrump Group, the Snowball Earth concept, microbialites, and the petrography of some Kingston Peak Formation eastern units.

Stratigraphy

Earlier studies have named the Neoproterozoic Pahrump Group and its three formations: Crystal Spring Formation (lower siliciclastic- carbonate unit), Beck Spring Dolomite (middle carbonate unit), and Kingston Peak Formation (upper siliciclastic unit) (Hewett, 1940; Miller, 1985; Petterson, 2009; Prave, 1999). Recently the upper member

of the Crystal Spring Formation was elevated to formation status and named the Horse Thief Springs Formation (Mahon et al., 2014). Table 1.1 shows the comparative stratigraphy of the Pahrump Group.

In the Death Valley region, the Pahrump Group occurs on the western side of Death Valley in the Panamint Range as a single large exposure and on the eastern side in isolated small ranges that are usually incomplete as compared to Panamint Range (Petterson, 2009). Below is a review of major features of each formation.

Beck Spring Dolomite

Beck Spring Dolomite (~100-600 m thick) consists of blue-gray dolostones with microbialites and oolitic packstones, occasional micrite, and minor siliciclastic interbeds. In the Kingston Range, the Beck Spring Dolomite is divided into four members: a lower laminated cherty member (~20-60 m thick), a laminated member with angular intraclasts and columnar stromatolites (~160-180 m thick), a relatively thinner oolitic-pisolitic member (~60-70 m thick), and a partially silicified upper member with abundant chert, shale lenses and stromatolites (~150-180 m thick) (Gutstadt, 1968; Marian and Osborne, 1992). Beck Spring Dolomite has been interpreted as an assemblage deposited in a shallow marine carbonate environment (Corsetti et al., 2003; Marian and Osborne, 1992).

Table 1.1. Comparative Stratigraphy of the Pahrump Group in western and eastern regions. Modified from (Macdonald et al., 2013; Mahon et al., 2014; Miller, 1985; Mrofka, 2010; Petterson, 2009; Prave, 1999). Formation names are aligned vertically and member and sub member names horizontally (except South Park member).

		WESTERN REGION (PANAMINT MOUNTAINS)			EASTERN REGION			
		Miller, 1985	Prave, 1999	Petterson, 2009	Prave, 1999	McDonald et al 2013	Mrofka 2010	Mahon et al 2014
PAHRUMP GROUP	NEOPROTEROZOIC CRYOGENIAN	KINGSTON PEAK FM Wildrose Mountain Girl Middle Park	KINGSTON PEAK FM South Park Wildrose Mountain Girl Middle Park	KINGSTON PEAK FM Wildrose Thorndike Mountain Girl Argenta Middle Park	KINGSTON PEAK FM Kp3	KINGSTON PEAK FM Kp4 Kp3	KINGSTON PEAK FM Jupiter Mine Silver Rule Mine	KINGSTON PEAK FM Kp4 Kp3
		Sourdough Ls Suprise mbr Limekiln Spring	Sourdough Ls Suprise Limekiln Spring	Sourdough Ls Suprise Limekiln Spring	Kp2 Kp1	Kp2 Kp1	Alexander Hills Diamictite Saratoga Hill Sandstone	Kp2 Kp1
	CRYSTAL SPRING FM	CRYSTAL SPRING FM	CRYSTAL SPRING FM	CRYSTAL SPRING FM	CRYSTAL SPRING FM	CRYSTAL SPRING FM	CRYSTAL SPRING FM	CRYSTAL SPRING FM
	MESO- TEROZOIC STENIAN	BECK SPRING DOLOMITE	BECK SPRING DOLOMITE	BECK SPRING DOLOMITE	BECK SPRING DOLOMITE	BECK SPRING DOLOMITE	BECK SPRING DOLOMITE	BECK SPRING DOLOMITE
		CRYSTAL SPRING FM	CRYSTAL SPRING FM	CRYSTAL SPRING FM	CRYSTAL SPRING FM	CRYSTAL SPRING FM	CRYSTAL SPRING FM	CRYSTAL SPRING FM HORSE THIEF SPRING FM
								Middle mbr Lower mbr

Kingston Peak Formation (KPF)

The Kingston Peak Formation crops out in two broad regions of western and eastern Death Valley (Miller, 1985). In the western region, the KPF crops out in a 120 km² area in the Panamint Range (Mrofka, 2010). Here the KPF has been subdivided into four members, from oldest to youngest: The Limekiln Spring, Surprise, Sourdough, and South Park (Labotka et al., 1980; Miller, 1985; Prave, 1999). In the Panamint Range, the South Park member has four sub-members, first identified by Murphy (1932). From

oldest to youngest they are the Middle Park, Mountain Girl, Thorndike, and Wildrose sub-members. Some studies have subdivided KPF in the Panamint Range into the Limekiln Spring, Surprise, Sourdough, Middle Park, Argenta, Mountain Girl, Thorndike (also referred to as the “unnamed” limestone), and Wildrose members (Petterson, 2009; Petterson et al., 2011). The Surprise member has been suggested to represent Sturtian glacial deposition and the Wildrose member represents Marinoan glacial deposition (Petterson et al., 2011; Prave, 1999).

In eastern Death Valley, the KPF crops out throughout a $70 \times 35 \text{ km}^2$ area in a number of ranges and hills (Mrofka, 2010). It consists of three informal units, KP₁, KP₂, and KP₃, a locally developed fourth unit, KP₄ (Macdonald et al., 2013; Mahon et al., 2014; Prave, 1999), and a unique limestone unit, the Virgin Spring Limestone which is between KP₁ and KP₂ (Macdonald et al., 2013; Tucker, 1986). Mrofka, (2010) has proposed specific informal names for KP₁- KP₄ in the eastern region: KP₁-Saratoga Hills Sandstone, KP₂-Alexander Hills Diamictite, KP₃- Silver Rule Mine, and KP₄- Jupiter Mine (Table1.1).

KP₁

KP₁ (~60- 250 m thick) represents a clear change in lithology from stromatolitic, oncolitic, and oolitic carbonates of the underlying Beck Spring Dolomite to a fine-grained siliciclastic that is also different from the coarse-grained lithologies of other KPF units (Macdonald et al., 2013; Mrofka, 2010). KP₁ has been described as preglacial with no diamictite (Corsetti et al., 2003).

It has been characterized by planar mm-scale parallel laminations, rare gentle cross-lamination, massive unlaminated thick beds, and beds with gently scoured bases and pock-marked and wavy textures on bedtops that resemble microbial mat surfaces (Mrofka, 2010). Some studies have suggested that KP₁ should be removed from the Kingston Peak Formation and be part of the Beck Spring Dolomite depositional cycle (Macdonald et al., 2013; Mrofka, 2010; Prave, 1999).

KP₂, KP₃ and KP₄

KP₂ (~50-370 m thick) contains the first coarse-grained deposit of cobble-to-boulder diamictite with lesser intervals of laminated and cross-laminated siltstones; it contains clasts from the underlying Virgin Spring limestone in some locations (Macdonald et al., 2013; Mrofka, 2010). KP₃ varies in thickness from few tens of meters to several kilometers. It has clasts similar to KP₂ but is dominated by clasts derived from the Beck Spring Dolomite, the Crystal Spring Formation, and probably the Horse Thief Springs Formation. It consists of several interbedded lithologies of iron-rich beds, olistolith-bearing diamictite, conglomerate, sandstone, siltstone, oncolite beds, and a rich microfossil assemblage (Corsetti et al., 2003; Macdonald et al., 2013; Mrofka, 2010). KP₄ (~2-30 m thick) contains additional layers of massive diamictite, which overlies KP₃ (Macdonald et al., 2013).

Beck Spring Dolomite - Kingston Peak Formation Boundary

Researchers in the Pahrump Group have defined BSD-KPF boundary using lithology change (Macdonald et al., 2013; Miller, 1985; Mrofka, 2010; Prave, 1999).

In this study BSD-KPF boundary is defined by an abrupt change in lithology. Depending on the locality, the contact between BSD and KPF in the Panamint Range has been described as conformable, inter-fingering and unconformable (Miller, 1985).

In the Eastern side of the Death Valley, the BSD-KPF contact has been described as gradational by some workers (Macdonald et al., 2013; Prave, 1999). In the Alexander Hills and Saratoga Hills, the BSD-KPF contact has been described as transitional and in the southern Black Mountains it has been described as sharp contact (Mrofka and Kennedy, 2011).

Geological Setting

The Pahrump Group provides a tectonic record of the supercontinent Rodinia; its rifting and general reconstruction together with the evolution of the western Laurentian margin (Fedo and Cooper, 2001; Mahon, 2012; Mahon et al., 2014; Miller, 1987; Petterson, 2009; Prave, 1999; Stewart, 1972).

Syn-depositional faults and mafic magmatism that have been observed in the Kingston Peak Formation suggest that it is a synrift deposit in an extensional basin that was created during the rifting of the western margin of Laurentia (Mahon et al., 2014; Mrofka, 2010; Prave, 1999). The Kingston Peak Formation has abrupt sedimentary facies and thickness changes across the basin suggesting that it was deposited in an actively extending tectonic setting (Corsetti and Kaufman, 2003; Prave, 1999)

Geochronology

The geochronology of the Pahrump Group has not been refined adequately. Most ages assigned have been based on regional and global correlations of lithostratigraphy

and chemostratigraphy (Dehler et al., 2010; MacLean, 2007; Mahon, 2012; Prave, 1999). So far, there are few direct radiometric age constraints on the Pahrump Group. One of them is from two U-Pb ages of 1069 ± 3 Ma and 1087 ± 3 Ma from baddeleyite in diabase sills in the lower and middle Crystal Spring Formation (Heaman and Grotzinger, 1992).

Recently, a comprehensive LA-ICPMS detrital zircon data set was published on the Pahrump Group in the clastic units of the Horse Thief Springs Formation that overlie a major unconformity above the Crystal Spring Formation with a maximum depositional age of 787 ± 11 Ma (Mahon et al., 2014).

Brief History of Research

The Neoproterozoic glacial units of the Kingston Peak Formation in the Panamint Range was first described in detail by Murphy in 1930-1932. He named the unit informally from bottom to top as Surprise Formation, Sourdough Limestone, Middle Park Formation and Wildrose Formation. He placed all the formations in the Telescope Group. These names, except Telescope Group, have been maintained and formalized to member status with the Telescope Group now called the Kingston Peak Formation (Mrofka, 2010).

Hewett, (1940) was the first to define the Pahrump Group in Death Valley with no type section descriptions. He proposed that the group consists of three formations: Crystal Spring Formation (lower siliciclastic- carbonate unit), Beck Spring Dolomite (middle carbonate unit) and Kingston Peak Formation (upper siliciclastic unit). More detailed stratigraphic studies followed (Miller, 1985; Prave, 1999; Wright et al., 1976)

and most recently the upper unit of the Crystal Spring Formation was elevated to be the Horse Thief Springs Formation (Mahon et al., 2014; Petterson, 2009).

Studies in the Pahrump Group have primarily focused on stratigraphy, sedimentology, and paleogeography (Corsetti and J. Kaufman, 2003; Mrofka, 2010; Prave, 1999; Topping, 1993; Walker et al., 1986; Wright et al., 1976), glaciation (Miller, 1985; Miller, 1987; Mrofka, 2010; Petterson, 2009), and microbialites (Corsetti et al., 2003; Horodyski and Mankiewics, 1990; Macdonald et al., 2013).

Snowball Earth

The global occurrences of late Neoproterozoic diamictite deduced to be of glacial origin can be explained by the Snowball Earth hypothesis (Hoffman et al., 1998; Hoffman and Schrag, 2002; Kirschvink, 1992). The Neoproterozoic Pahrump Group of the Death Valley area, records two low-latitude glaciations that have been studied extensively (Corsetti and J. Kaufman, 2003; Miller, 1985; Prave, 1999). A glaciogenic origin has been proposed for three units within the Kingston Peak Formation in the Panamint Range: The Limekiln Spring Member, the Surprise Member, and the Wildrose Sub-member (Miller, 1985; Petterson, 2009).

Convincing evidence for a glacial origin in Kingston Peak Formation has been primarily from the eastern region, where striated and faceted clasts have been reported (Miller, 1985; Mrofka, 2010). Evidence for glaciation within the Kingston Peak Formation in the Panamint Range (western region) is mostly indirect (Petterson, 2009).

Kingston Peak Formation diamictites in the western region have been placed within the Sturtian and Marinoan glacial intervals (Figure 1.1) with the Surprise member

representing a Sturtian glacial deposit and Wildrose member a Marinoan glacial deposit (Pettersen, 2009).

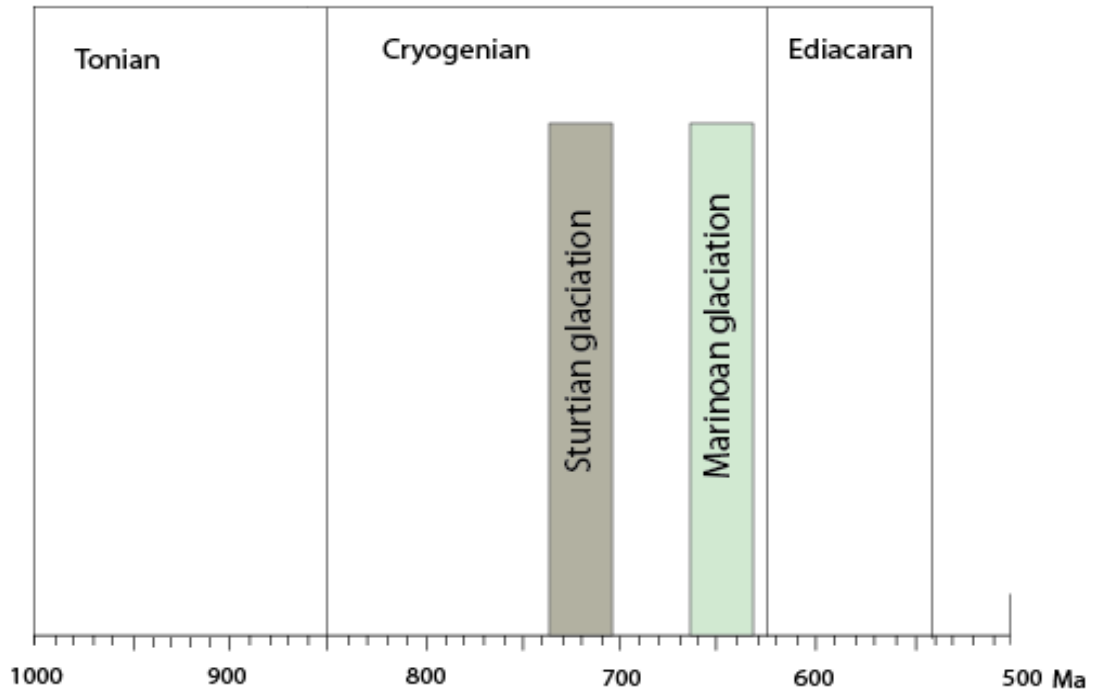


Figure 1.1. Two major glaciations during Neoproterozoic time. Modified from (Hoffman and Schrag, 2002).

Microbialites

The Neoproterozoic Era record suggests a major diversification of biotas and extreme changes in climate, including Snowball Earth events (Corsetti et al., 2003; Hoffman et al., 1998; Horodyski and Mankiewicz, 1990; Kirschvink, 1992). The severity of Snowball Earth conditions has been questioned especially within the paleobiology community (Corsetti et al., 2003).

Few microfossils have been reported before, during, and after Snowball Earth times (Corsetti et al., 2003). Neoproterozoic microfossils have been described from the Beck Spring and Kingston Peak Formations in the eastern Death Valley region (Corsetti et al., 2003; Horodyski and Mankiewics, 1990). At least 12 distinctive microfossil morphotypes have been reported within the Beck Spring Dolomite and the Kingston Peak Formation (Corsetti et al., 2003).

There is no report of microfossils from Pahrump Group strata in the Panamint Range probably due to the high degree of metamorphism. But even unmetamorphosed strata elsewhere lack microfossils (Corsetti et al., 2003; Petterson, 2009). Complex microfossils preserved in chert and carbonate has been described from the oncolitic dolostone bed within KP₃ with similar microfossils are also identified in chert nodules from the Beck Spring Dolomite (Corsetti et al., 2003; Mrofka, 2010).

Petrography of Kingston Peak Subunits

KP₁

The only detailed petrographic descriptions of units in the Kingston Peak in the eastern region are from Mrofka (2010). Sandstones have various grain-to-grain relationships and matrices. Grains are angular to sub-angular and a few are sub-rounded. All have poor sorting (Mrofka, 2010). Some sandstone beds are grain supported and others matrix supported. Matrix material is mostly composed of quartz silt and clay, but can also be carbonate or carbonate-rich at the base of KP₁ near the gradational contact with the Beck Spring Dolomite and also at the top of the member. He also observed that lithic grains are common in many beds. Mrofka (2010).

KP₂

Grains are sub-rounded to very-angular and poorly sorted and dominated by quartz with some feldspar and lithic grains. Matrix material is very fine quartz sand, greenish-yellow clay, or carbonate. Toward the base, the diamictite contains a higher percentage of Virgin Spring Limestone clasts and the diamictite matrix is more typically dark black and carbonate-rich (Mrofka, 2010).

KP₃

Thin sections studied reveal that sandstone beds and matrix of diamictite beds are both compositionally and physically immature. Quartz grains are poorly sorted and sub-rounded to very angular. Some beds have calcite cement and others contain grains of carbonate. Diamictite beds in the upper *KP₃* are similar to the diamictite in the underlying *KP₂* member. They contain clasts of the Virgin Spring Limestone including the characteristic spherules (Mrofka, 2010).

KP₄

Most *KP₄* beds have debrites and sedimentary breccias that are compositionally and physically immature. Some beds have carbonate-rich matrices with grains more rounded than in the underlying *KP₃* but very poorly sorted. Lithic grains are common (Mrofka, 2010).

References

- Corsetti, F. A., Awramik, S. M., and Pierce, D., 2003, A complex microbiota from snowball Earth times: microfossils from the Neoproterozoic Kingston Peak Formation, Death Valley, USA: *Proc Natl Acad Sci USA*, v. 100, no. 8, p. 4399-4404.
- Corsetti, F. A., and J. Kaufman, A., 2003, Stratigraphic investigations of carbon isotope anomalies and Neoproterozoic ice ages in Death Valley, California: *Geological Society of America Bulletin*, v. 115, no. 8, p. 916-932.
- Dehler, C. M., Fanning, C. M., Link, P. K., Kingsbury, E. M., and Rybczynski, D., 2010, Maximum depositional age and provenance of the Uinta Mountain Group and Big Cottonwood Formation, northern Utah: *Paleogeography of rifting western Laurentia: Geological Society of America Bulletin*, v. 122, no. 9-10, p. 1686-1699.
- Fedo, C. M., and Cooper, J. D., 2001, Sedimentology and sequence stratigraphy of Neoproterozoic and Cambrian units across a craton-margin hinge zone, southeastern California, and implications for the early evolution of the Cordilleran margin: *Sedimentary Geology*, v. 141, p. 501-522.
- Gutstadt, A. M., 1968, Petrology and depositional environments of the Beck Spring dolomite (Precambrian), Kingston Range, California: *Journal of sedimentary petrology*, v. 38, no. 4, p. 1280-1289.
- Heaman, L. M., and Grotzinger, J. P., 1992, 1.08 Ga diabase sills in the Pahrump Group, California: Implications for development of the Cordilleran miogeocline: *Geology*, v. 20, no. 7, p. 637.
- Hewett, D. F., 1940, New formation names to be used in the Kingston Range, Ivanpah quadrangle, California: *Washington Academy of Sciences*, v. 30, no. 6, p. 239-240.
- Hoffman, P. F., Kaufman, A. J., and Halverson, G. P., 1998, Comings and goings of global glaciations on a Neoproterozoic tropical platform in Namibia: *Geological society of America* v. 8, no. 5.
- Hoffman, P. F., and Schrag, D. P., 2002, The snowball Earth hypothesis: testing the limits of global change: *Terra Nova*, no. 14, p. 129-155.
- Horodyski, R. J., and Mankiewics, C., 1990, Possible Late Proterozoic skeletal algae from the Pahrump Group, Kingston Range, Southeastern California: *American Journal of science*, v. 290-A, no. 149-169.

- Kirschvink, J. L., 1992, A paleogeographic model for Vendian and Cambrian time: The Proterozoic biosphere: A multidisciplinary study: Cambridge University Press, p. 569-581.
- Labotka, T. C., Albee, A. L., Lanphere, M. A., and McDowell, S. D., 1980, Stratigraphy, structure, and metamorphism in the central Panamint Mountains (Telescope Peak quadrangle), Death Valley area, California: Summary: Geological Society of America Bulletin, v. 91, no. 3, p. 125.
- Lloyd, S. J. s., and Corsetti, F. A., 2010, The origin of the millimeter-scale lamination in the Neoproterozoic lower Beck Spring Dolomite: Implications for widespread, fine scale, layer-parallel diagenesis in Precambrian carbonates: Journal of Sedimentary Research, v. 80, no. 7-8, p. 678-687.
- Macdonald, F. A., Prave, A. R., Petterson, R., Smith, E. F., Pruss, S. B., Oates, K., Waechter, F., Trotsuk, D., and Fallick, A. E., 2013, The Laurentian record of Neoproterozoic glaciation, tectonism, and eukaryotic evolution in Death Valley, California: Geological Society of America Bulletin, v. 125, no. 7-8, p. 1203-1223.
- Mahon, R. C., 2012, Detrital Zircon Provenance, Geochronology and Revised Stratigraphy of the Mesoproterozoic and Neoproterozoic Pahrump (Super) Group, Death Valley Region, California and Geology of the Saddle Peak Hills 7.5' Quadrangle, San Bernardino County, California [M.S. thesis]: Idaho State University.
- Mahon, R. C., Dehler, C. M., Link, P. K., Karlstrom, K. E., and Gehrels, G. E., 2014, Geochronologic and stratigraphic constraints on the Mesoproterozoic and Neoproterozoic Pahrump Group, Death Valley, California: A record of the assembly, stability, and breakup of Rodinia: Geological Society of America Bulletin.
- Marian, M. L., and Osborne, R. H., 1992, Petrology, petrochemistry, and stromatolites of the Middle to Late Proterozoic Beck Spring Dolomite, eastern Mojave Desert, California: Canadian Journal of Earth Sciences, v. 29, p. 2595-2609.
- Miller, J. M. G., 1985, Glacial and syntectonic sedimentation: The upper Proterozoic Kingston Peak Formation, southern Panamint Range, eastern California: Geological Society of America Bulletin, v. 96, no. 12, p. 1537.
- Miller, J. M. G., 1987, Paleotectonic and stratigraphic implications of the Kingston Peak-Noonday contact in the Panamint Range, eastern California: Journal of Geology, v. 95, no. 1, p. 75-85.
- Mrofka, D. D., 2010, Competing Models for the Timing of Cryogenian Glaciation: Evidence from the Kingston Peak Formation, Southeastern California [Ph.D. thesis]: Riverside, California, University of California at Riverside.

- Petterson, R., 2009, Glacigenic and related strata of the Neoproterozoic Kingston Peak Formation in the Panamint Range, Death Valley region, California. II. The basal Ediacaran Noonday Formation, eastern California, and implications for Laurentian equivalents. III. Rifting of southwest Laurentia during the Sturtian–Marinoan interglacial: The Argenta Orogeny [Ph.D. thesis]: California Institute of Technology.
- Petterson, R., Prave, A. R., Wernicke, B. P., and Fallick, A. E., 2011, The Neoproterozoic Noonday Formation, Death Valley region, California: Geological Society of America Bulletin, v. 123, no. 7-8, p. 1317-1336.
- Prave, A. R., 1999, Two diamictites, two cap carbonates, two delta C-13 excursions, two rifts: The Neoproterozoic Kingston Peak Formation, Death Valley, California: Geology, v. 27, no. 4, p. 339-342.
- Stewart, J. H., 1972, Initial Deposits in the Cordilleran Geosyncline: Evidence of a Late Precambrian (<850 m.y.) Continental Separation: Geological Society of America Bulletin, v. 83, no. 5, p. 1345.
- Topping, D. J., 1993, Paleogeographic reconstruction of the Death Valley extended region: Evidence from Miocene large rock-avalanche deposits in the Amargosa Chaos Basin, California: Geological Society of America Bulletin, v. 105, no. 9, p. 1190-1213.
- Tucker, M. E., 1986, Formerly aragonitic limestone associated with tillites in the Late Proterozoic of Death Valley, California: Journal of Sedimentary Petrology, v. 56, no. 6, p. 818-830.
- Walker, J. D., Klepacki, D. W., and Burchfiel, B. C., 1986, Late Precambrian tectonism in the Kingston Range, southern California: Geology, v. 14, no. 1, p. 15.
- Wright, L., A., Troxel, B. W., Williams, G. E., Roberts, M. T., and Diehl, P. E., 1976, Precambrian sedimentary environment of the Death Valley region, eastern California: California Division of Mines and Geology Special Report 106 p. 7-15.

CHAPTER TWO

**SEDIMENTOLOGY OF KINGSTON PEAK FORMATION KP₁ BEDS IN BECK
CANYON REGION, KINGSTON RANGE, CALIFORNIA**

Abstract

The Neoproterozoic Kingston Peak Formation (KPF) is known for its diamictites interpreted as of glacial origin. The KPF overlies the Beck Spring Dolomite (BSD) which contains microfossils and microbialites. This study aims to test correlation between outcrops and understand the abrupt change from BSD to KPF. It focuses on the basal 4 meters of the KP₁ subunit of the KPF as it appears in the Beck Canyon region, Kingston Range, California. We describe and correlate sedimentary rocks at and immediately overlying the contact and analyze the sedimentary structures, textures and sequences.

We have found only three sites in the northern Kingston Peak Range where the contact can be observed. At each site we measured sections about 4 meters long across the contact. The top of the BSD in all locations contains microbial laminations, oncoids, pisoids, sheets of chert and peloids. Thin sections from about 15 cm below the contact to about 50 cm above the contact show microbial laminations with some peloids or ghosts of peloids and abundant chert. The base of the KPF is composed of two bed types named A-bed and B-bed. A-beds are clastic-rich and B-beds are dolomite-rich. A-beds are dolomitic silty mudstones with abundant muscovite. B-beds are recrystallized silty dolostones with peloid ghosts. A few of the beds show faint current ripple cross bedding, cross bedding and lenticular structures. A-bed to B-bed contacts are sharp. At all stratigraphic levels, clastics have immature textures and composition. XRD and thin section analysis show a trend of decreasing dolomite up-section. Measurement and

analysis of individual alternating bed thickness show cyclical patterns and a gradational increase in bed thickness to massive sandstones.

Mineralogical patterns, pisoid-rich layers, and bed thickness patterns can all be correlated among the three sections. The pattern of increasing clastic content and bed thickness upsection suggests clastic influx during progradation that progressively overwhelmed carbonate production. This progradational setting could have occurred on a tide dominated delta or on a prograding tidal flat. The BSD-KPF contact at Kingston Range most likely represent a sequence boundary as evidenced by a change in lithology from dolostones to clastics.

Introduction

The Neoproterozoic Beck Spring Dolomite and Kingston Peak Formation are part of the Pahrump Group of the Death Valley area, California. The Pahrump Group contains an important geologic record for understanding rifting of the super-continent Rodinia, biotic evolution, evolution of the western Laurentian margin, and extreme global climate change, which includes snowball Earth (Fedo and Cooper, 2001; Labotka et al., 1980; Miller, 1985; Petterson, 2009; Prave, 1999).

Although some gradual transitions between the BSD and KPF has been reported in the eastern side of the Pahrump Group, in the Saratoga Hills Sandstone there is an abrupt change in lithology from dolostones in the BSD to sandstones in the KPF (Mrofka, 2010). Detailed sedimentologic studies have not been carried out in the areas with these abrupt changes. This project seeks to understand the abrupt change from BSD to KPF as it appears in three localities with the Beck Canyon region, Kingston Range, California (Figures 2.1 and 2.2).

Geologic Setting

The Pahrump Group contains an important geologic record of the super-continent Rodinia that helps to understand its rifting and general reconstruction together with the evolution of the western Laurentian margin (Fedo and Cooper, 2001; Mahon, 2012; Mahon et al., 2014; Miller, 1987; Petterson, 2009; Prave, 1999; Stewart, 1972).

Evidence for continental rifting within the Pahrump Group has been documented primarily from the Kingston Peak Formation (Petterson, 2009; Walker et al., 1986). The relation of other Pahrump Group units to the rift history in the region has not been adequately explored (Mahon, 2012)

Syn-depositional faults and mafic magmatism that have been observed in the Kingston Peak Formation suggest that it is a synrift deposit in an extensional basin that was created during the rifting of the paleo-western margin of North America (Mahon et al., 2014; Mrofka, 2010; Prave, 1999). The Kingston Peak Formation has abrupt sedimentary facies and thickness changes across the basin suggesting that it was deposited in an actively extending tectonic setting (Corsetti and Kaufman, 2003; Prave, 1999).

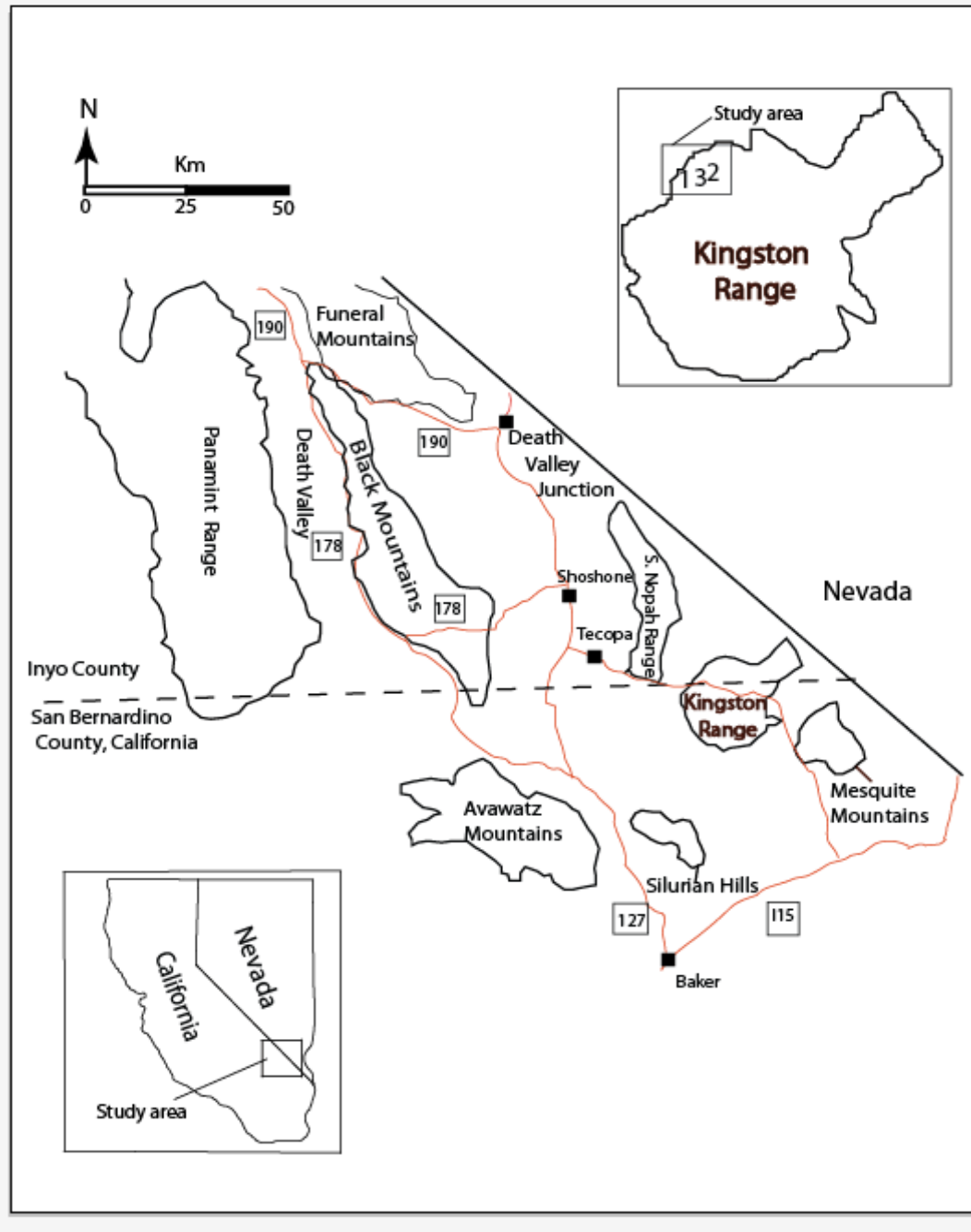


Figure 2.1. Map showing the study area in context of surrounding mountain ranges. The red lines show the highways in the region and the dotted lines show county boundaries. Modified from (Mrofka, 2010).

Stratigraphy

The Neoproterozoic Pahrump Group was traditionally divided into three formations: Crystal Spring Formation, Beck Spring Dolomite, and Kingston Peak Formation (Hewett, 1940; Miller, 1985; Petterson, 2009; Prave, 1999). Recently, the upper member of Crystal Spring Formation was elevated to formation status and named the Horse Thief Springs Formation (Mahon et al., 2014). Table 1.1 shows the comparative stratigraphy of the Pahrump Group.

In the Death Valley region, the Pahrump Group occurs on the western side in the Panamint Range as a single large exposure and on the eastern side of Death Valley in isolated small ranges that are usually incomplete as compared to Panamint Range (Petterson, 2009).

Beck Spring Dolomite

The Beck Spring Dolomite consists of blue-gray dolostones with microbialite, oolitic packstone, occasional micrite, and minor siliciclastic interbeds. In the Kingston Range, the Beck Spring Dolomite is divided into four members: a lower laminated cherty member, a laminated member with angular intraclasts and columnar stromatolites, a relatively thinner oolitic-pisolitic member, and a partially silicified upper member with abundant chert, shale lenses, and stromatolites (Gutstadt, 1968; Marian and Osborne, 1992).

Kingston Peak Formation (KPF)

The Kingston Peak Formation crops out in two broad regions on the western and eastern sides of Death Valley (Miller, 1985). In the western region, KPF occurs in the

Panamint Range. Here KPF has been subdivided into four members, from oldest to youngest the Limekiln Spring, Surprise, Sourdough, and South Park (Labotka et al., 1980; Miller, 1985; Prave, 1999). Several other subdivisions have been assigned and they are documented in Table 1.1.

In eastern Death Valley, the KPF consists of informal units, KP₁, KP₂, and KP₃, a locally developed fourth unit, KP₄ (Macdonald et al., 2013; Mahon et al., 2014; Prave, 1999), and a unique limestone unit, the Virgin Spring Limestone, which is between KP₁ and KP₂ (Macdonald et al., 2013; Tucker, 1986). Mrofka, (2010) has proposed specific informal names for KP₁ – KP₄ in the eastern region: KP₁-Saratoga Hills Sandstone, KP₂-Alexander Hills Diamictite, KP₃- Silver Rule Mine and KP₄- Jupiter Mine (Table 1.1).

Beck Spring Dolomite - Kingston Peak Formation Boundary

Researchers in the Pahrump Group have defined the BSD-KPF boundary using lithology change (Macdonald et al., 2013; Miller, 1985; Mrofka, 2010; Prave, 1999). In this study the BSD-KPF boundary is also defined by an abrupt change in lithology. Depending on the locality, the contact between BSD and KPF in the Panamint Range has been described as conformable, inter-fingering and unconformable (Miller, 1985).

In the Eastern side of the Death Valley, the BSD-KPF contact has been described as gradational by some workers (Macdonald et al., 2013; Prave, 1999). In the Alexander Hills and Saratoga Hills, the BSD-KPF contact has been described as transitional and in the southern Black Mountains it has been described as sharp contact (Mrofka and Kennedy, 2011).

Methods

The first aim of this study is to correlate between locations so as to have confidence in comparing processes and environmental indicators. We located potential sites with the BSD-KPF contact by satellite views from Google™ earth, but eventually walked the entire contact on the north side of the Excelsior mine road. We compared sites by texture and composition through field observations and laboratory analyses. Correlation was strengthened above the contact by comparing trends in mineralogy, texture, and cycles in bedding patterns by detailed characterization using x-ray diffraction, thin section analysis, and SEM-EDS. For XRD analysis, samples were ground into fine particles of about 2-5 μm and then analyzed without using an added standard. Jade software, which uses an algorithm of whole pattern fitting to give semi-quantitative estimates of mineral percentages, was used to calculate mineral percentages. Thin alternating beds were measured in the field with a ruler to the nearest millimeter in approximately the lower four meters, beginning at the BSD-KPF contact.

The second aim of this study is to explain changes in depositional processes through time and trending away from the basal contact. All data collected were used to define facies. We analyzed those by describing sedimentary structures and bedding types in the field and collected samples that were slabbed and analyzed in the lab. Structures observed were described and photographed. Depositional processes have been inferred based on those facies. Trends were observed and analyzed after plotting all data.

Results

General Description of the Outcrop

Only three sites were identified within the northern Kingston Range having an exposed contact between the Beck Spring Dolomite and Kingston Peak Formation (Figures 2.2-2.4). The three locations are listed in Table 2.1. The contact between BSD and KPF is covered in most of the northern Kingston Range area. Where visible, the KPF is preferentially eroded compared to the top of the BSD. The top of the Beck Spring Dolomite in all three locations contains dolostones with wavy and crinkled microbial laminations, oncoids, pisoids, and light brown to black layers of chert.

Table 2.1. List of location coordinates for the areas studied.

Location (section)	Coordinates
1	35°47'54.32"N, 115°57'40.71"W.
2	35°48'30.25"N, 115°57'00.60"W.
3	35°48'32.91"N, 115°57'25.82"W.

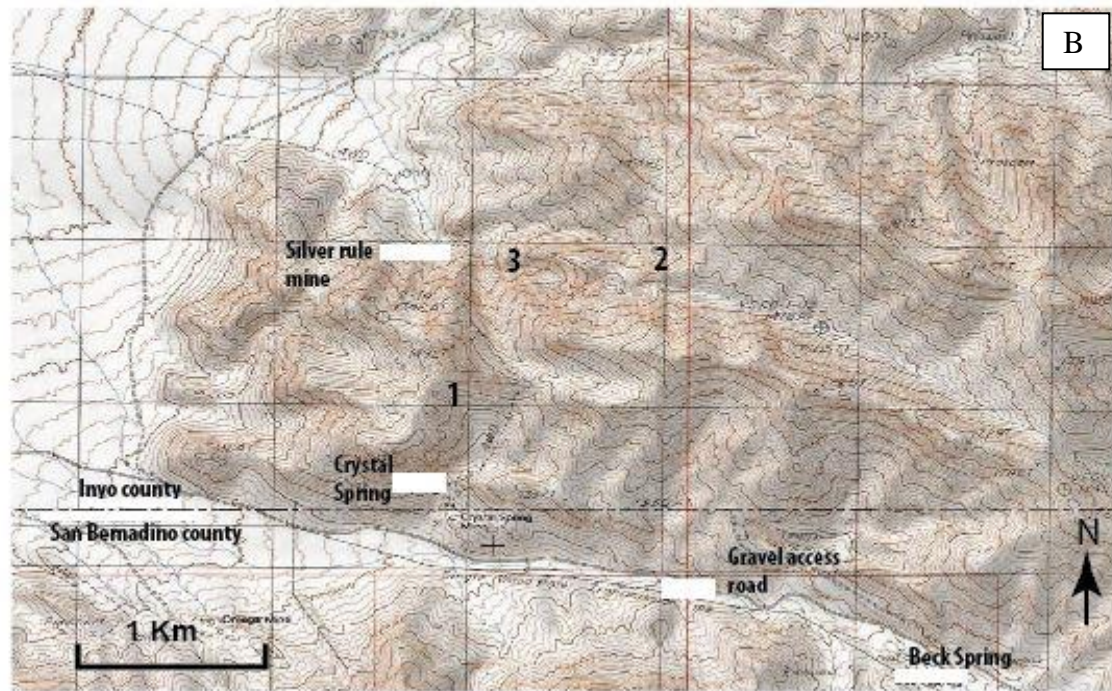


Figure 2.2. Google Earth and topographic maps showing the study area. (A) Google Earth map with the three localities studied. Red dashed lines in A show the KPF-BSD contact. Blue boxes are along the access road. (B) Topographic map with the three localities studied. The grid in B is 1km and important features and places are named. Location 1 is named Beck Canyon in the literature (Macdonald et al., 2013).

The general appearance of the studied interval shows the base of the Kingston Peak Formation is composed of millimeter to centimeter-scale alternating clastic-rich (A) and dolomite-rich (B) thick laminae and thin beds. These alternating beds consist of about 1.8m of thick laminae with a few thin beds followed by very few thick laminae and many thin beds. This produces a general pattern of thickening beds up-section. A few of the thin beds show faint current ripple cross bedding and lenticular structures.

The alternating thick laminae and thin beds are overlain by bedded, fine-grained sandstones showing only a few sedimentary structures including hints of cross bedding and planar partings every few meters. Bedding and parting surfaces in the sandstones are planar and flat (Figures 2.2-2.4). In the study areas, the first diamictites of the Kingston Peak Formation appear about 60 meters above the BSD-KPF contact.

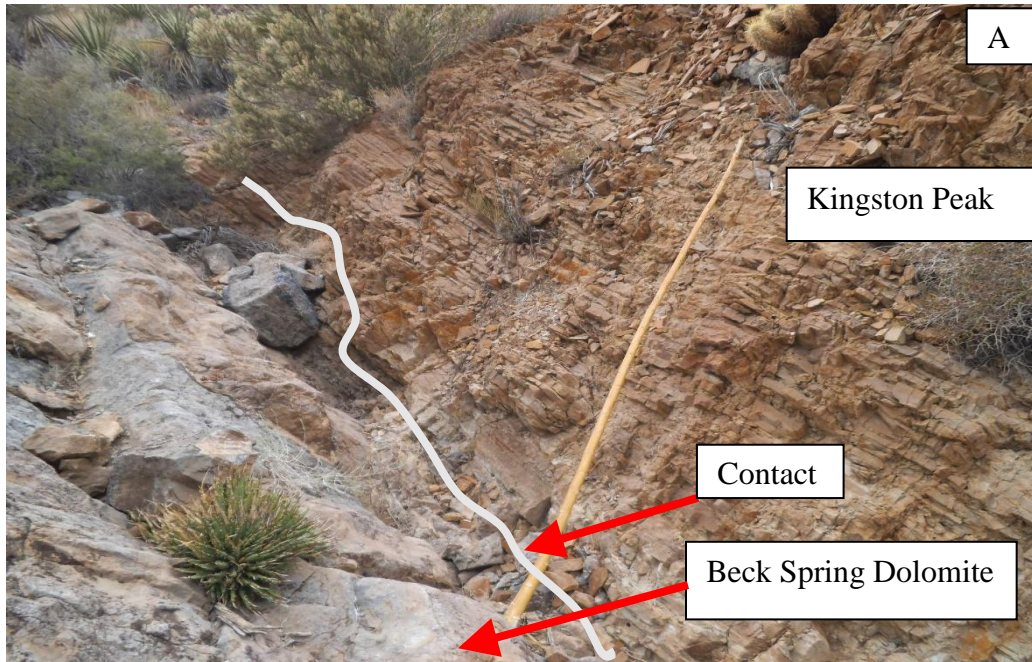


Figure 2.3. Field appearance at location 1. (A) Photograph shows the contact between Kingston Peak Formation and Beck Spring Dolomite. (B) Thin, alternating beds located at the base of Kingston Peak Formation. B-beds are gray in color while A-beds are brown in color. The contact at location 1 is clearer than other locations. Length of stick in (A) is about one meter.

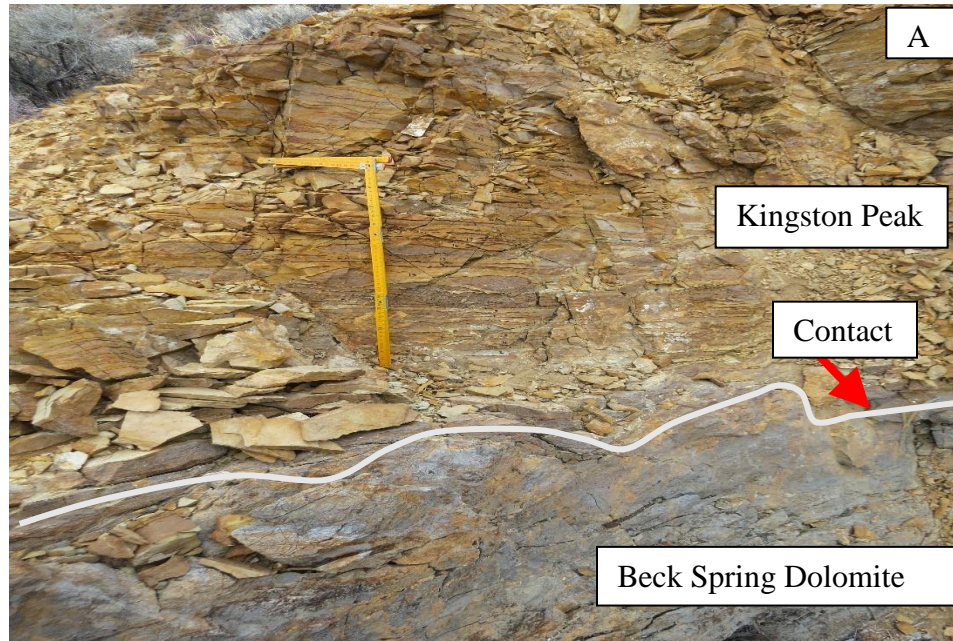


Figure 2.4. Field appearance at location 2. (A) The contact between Kingston Peak Formation and Beck Spring Dolomite. (B) Thin alternating beds at the base of Kingston Peak Formation. Numbers on the outcrop are to track the measurement of the thin beds.

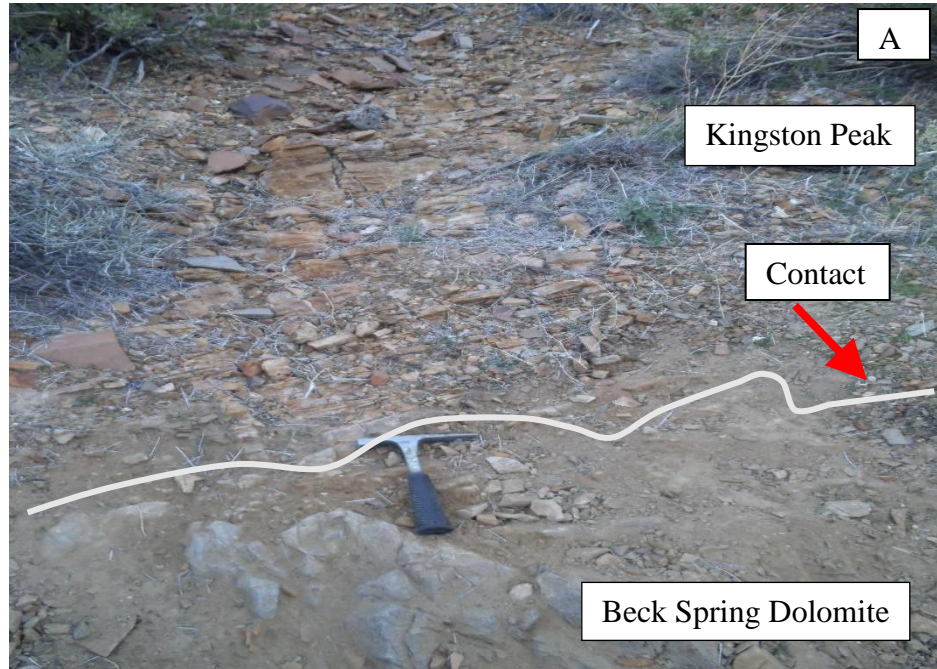


Figure 2.5. Field appearance at location 3. (A) The contact between Kingston Peak Formation and Beck Spring Dolomite. (B) Thin alternating beds at the base of Kingston Peak Formation.

Facies

We measured and correlated three sections, one from each location that includes the Kingston Peak-Beck Spring contact. Three facies were identified in each section, with one facies having sub-facies. Facies 1 is altered dolostone, facies 2 is interbedded dolostones and silty mudstones divided into subfacies of thinly interbedded silty dolostones and silty mudstones (2a) and thinly interbedded sandy dolostones and silty mudstones (2b), and facies 3 is fine sandstone with no visible internal sedimentary structures.

Facies 1: Altered Dolostones

This facies is at the top of the Beck Spring Dolomite where it is in contact with the Kingston Peak Formation (Figures 2.2, 2.3, and 2.4). This facies is generally characterized by light brown layers of chert, wavy and crinkled microbial laminations, peloids, oncoids, pisoids and fractures containing micro breccia (Figures 2.5, 2.6, and 2.7).

Dolomite is the dominant mineral in this facies with small amounts of quartz and feldspar. Small amounts of disseminated kaolinite are present. Detailed mineralogical data of this facies is presented in Tables 2.2-2.4. Dolomite crystals are generally subhedral (Figure 2.7) and show a moderately narrow range of crystal sizes (30 to 40 μm). No porosity was observed. Fractures containing clay and iron oxides are present.

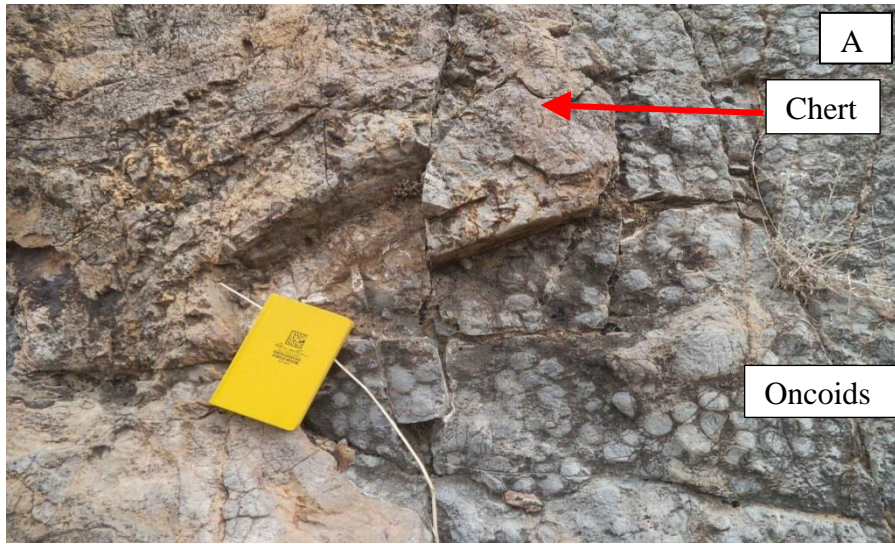


Figure 2.6. Photographs of the field appearance of facies 1 in location 1. (A) Bed with chert and oncoids. (B) Bed with grading pattern where there are small oncoids at the bottom and big oncoids at the top.



Figure 2.7. Photograph of the field appearance of facies 1 showing a bed with wavy and crinkled microbial laminations.

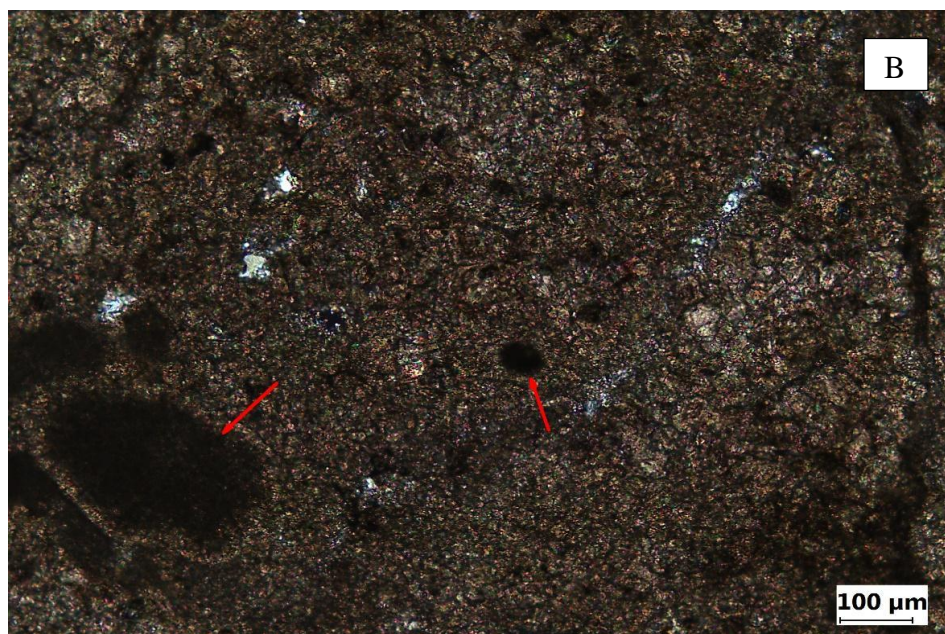
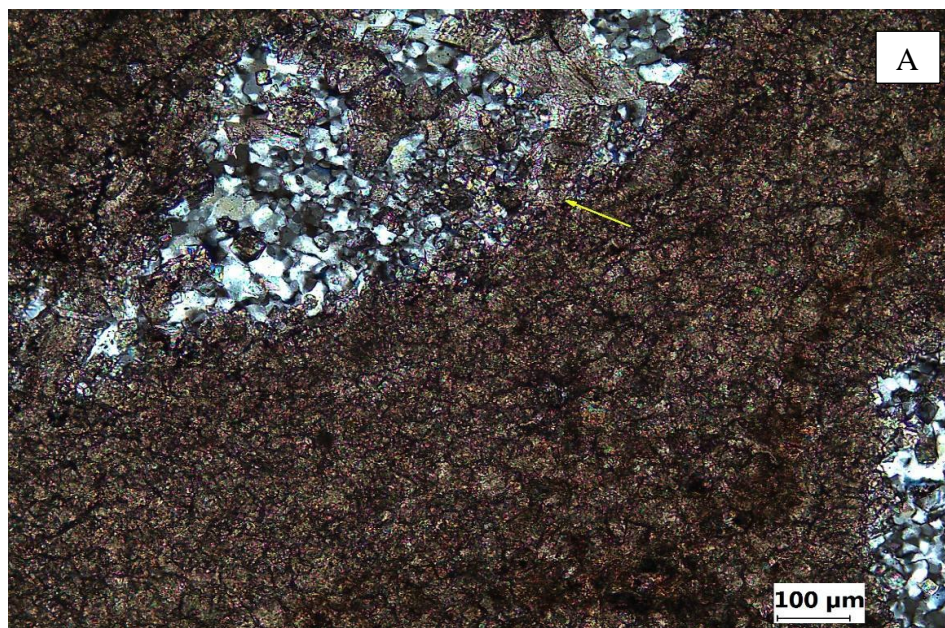


Figure 2.8. Photographs of facies 1 in thin section. (A) Chert replacing dolomite (yellow arrow). (B) Peloids (red arrows). Facies 1 is mostly dolomite.

Facies 2: Interbedded Dolostones and Silty Mudstones

Facies 2a: Thinly Interbedded Silty Dolostones and Silty Mudstones

This facies is stratigraphically above facies 1 (Figure 2.8). This facies contains two types of beds, called A-bed and B-bed. A-beds are dominated by clastic materials and B-beds are dominated by dolomite. In some cases, the contact between the two lithologies is sharp but in most cases it is gradational (Figure 2.9). The A and B thin beds of this facies have poorly sorted texture and no porosity. The sedimentary structures include: alternating thick laminae and thin beds with sub parallel contacts, subparallel laminations and faint ripple cross bedding (Figure 2.8 A).

Silt-size non-detrital dolomite crystals generally dominate the dolomitic (B-bed) portion of this facies with some peloidal ghosts defined by inclusions and a slight variation in crystal size. Crystal size range is 30 to 50 μm (Figure 2.9 A). Between some dolomite crystals are silt-size quartz crystals. There are some fractures in this unit, extending up to the clastic portion.

The clastic (A-bed) portion is generally poorly sorted and crystals are angular to sub angular. XRD mineralogical analysis of this portion indicates that the dominant minerals are quartz and feldspars with minor biotite, muscovite, and kaolinite. About 15% of the A-beds have a kaolinite-dominated matrix (Figure 2.9 A). Some fractures cross both A and B beds.



Figure 2.9. Photographs of typical field appearance of facies 2. (A) Many alternating thick laminae and few thin beds that are more planar, typical of facies 2a. (B) Many alternating thin beds with few thick laminae that are less planar, typical of facies 2b. The sedimentary structures in both 2a and 2b include; alternating thick laminae and thin beds, sub parallel laminations and faint ripple cross bedding.

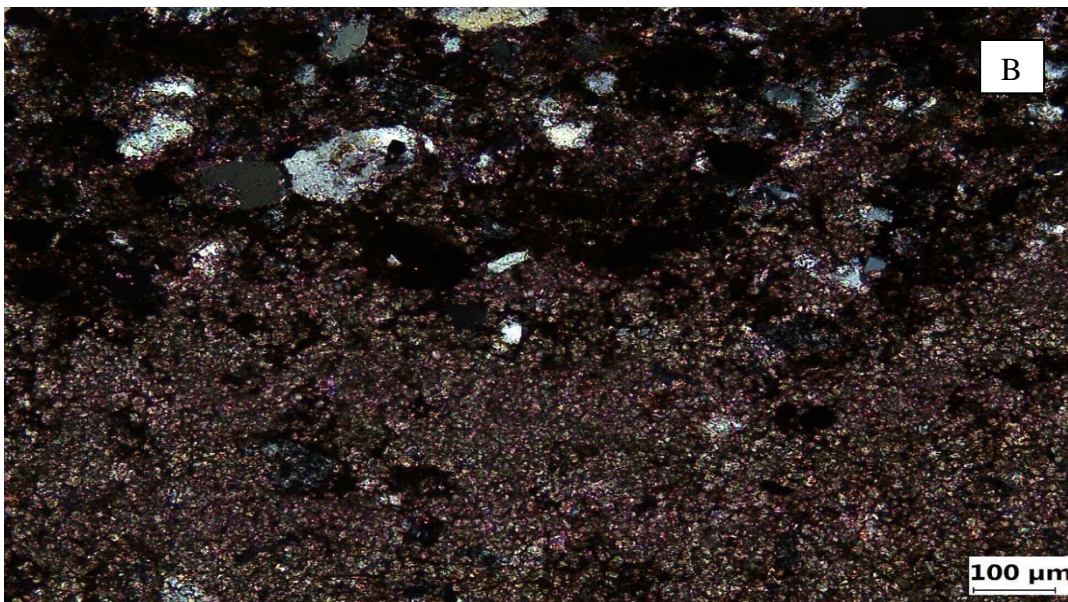
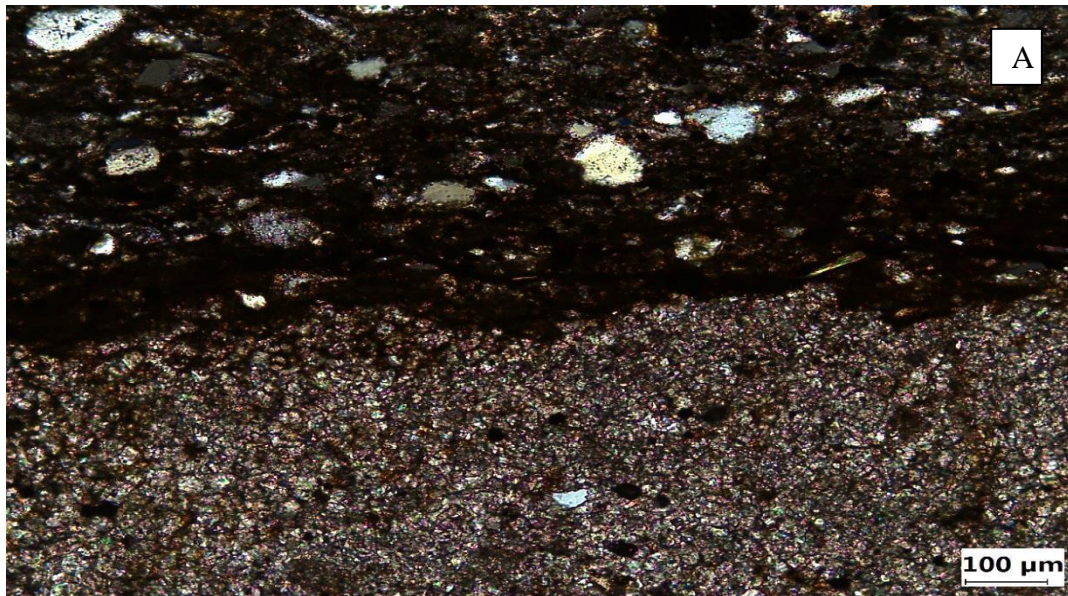


Figure 2.10. Photographs of facies 2 lithologies in thin section. Two examples of contacts between A and B beds are shown. (A) Sample with silt sized quartz grains with a sharp contact typical facies 2a. (B) Sample with some sand sized quartz grains with a less sharp contact typical of facies 2b.

Facies 2b: Thinly Interbedded Sandy Dolostones and Silty Mudstones

This facies is above 2a and it contains two types of beds, called A-bed and B-bed. A-beds are dominated by clastic materials and B-beds are dominated by dolomite. The contact between the two lithologies is gradational. Sedimentary particles in this facies are poorly sorted and the rocks preserve no porosity. This facies is different from facies 2a due to its many sand sized quartz grains in the dolomitic (B-beds). Sedimentary structures include: thick laminae to thin beds with subparallel contacts, and a few examples of faint cross bedding. A few laminae locally have rippled or low amplitude dune shapes with subparallel internal laminae (Figure 2.8 B).

The dolomite portion of this facies is generally dominated by subhedral dolomite crystals. The dolomite contains some sand-size quartz grains. Crystal size range is 40 to 60 μm (Figure 2.9 B). Clastic beds are generally poorly sorted and detrital grains are angular to sub-angular (Figure 2.9 B). XRD analysis indicates that the dominant minerals are quartz and feldspars, with minor muscovite and kaolinite. Most of the matrix is kaolinite.

Facies 3: Bedded Fine Sandstones

This facies is at the top of the sections that we measured in all locations, above sub-facies 2b. It is characterized by the absence of dolostone, abundance of fine sand, and the absence of internal stratification. The facies is poorly sorted and shows no porosity. There are no visible internal sedimentary structures (Figure 2.10)

XRD analysis of this facies indicates that the dominant minerals are quartz and feldspars with muscovite, illite, and kaolinite. The matrix is generally about 20% of the rock volume and is made up of illite and kaolinite (Figures 2.11 and 2.12).



Figure 2.11. Photographs of field appearance of facies 3. It is a fine sandstone in thick to very thick beds. The facies has no visible internal sedimentary structures.

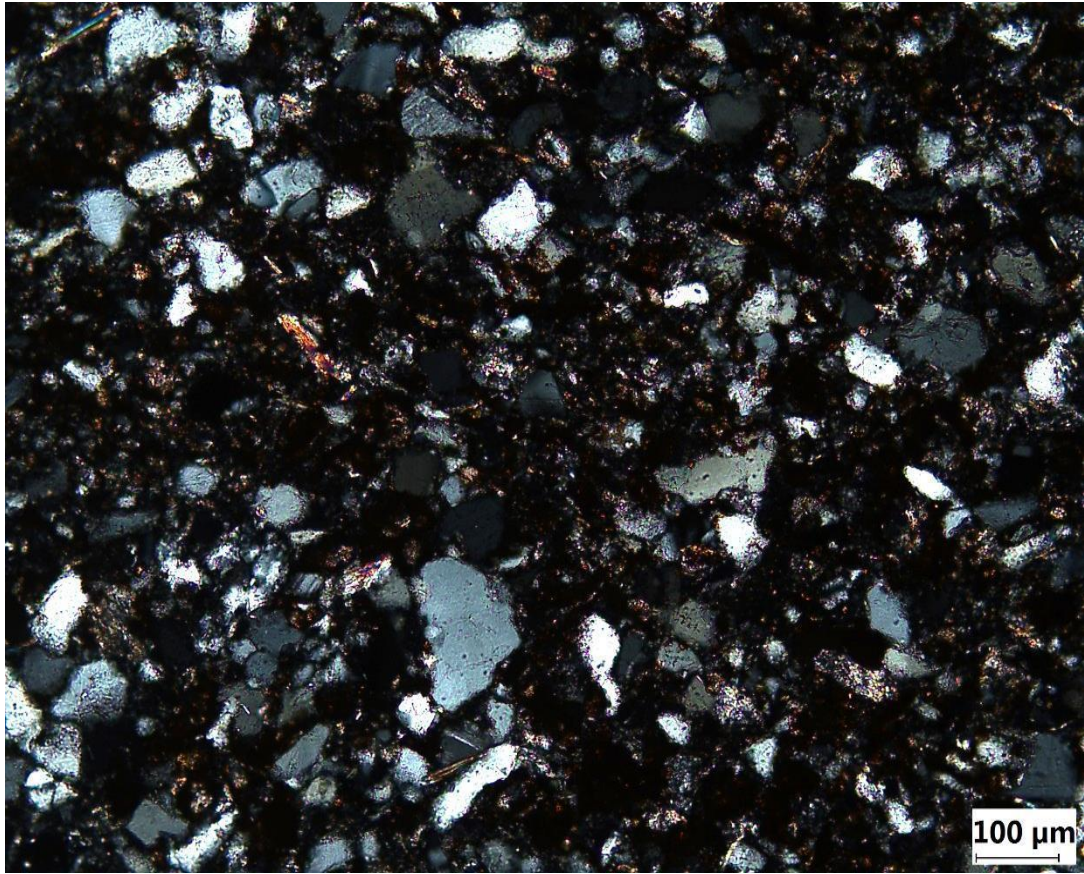


Figure 2.12. Photographs of facies 3 in thin section from location 1. The facies is made up of poorly sorted fine sandstone with abundant quartz grains that are angular to sub-angular with abundant matrix. Most of the grains exhibit unit (non undulatory) extinction. A few grains exhibit slight undulatory extinction. Most quartz grains occur as single crystals; polycrystalline quartz grains are generally rare. This facies contains entirely clastic materials which include quartz, feldspars, mica (muscovite) and clay.

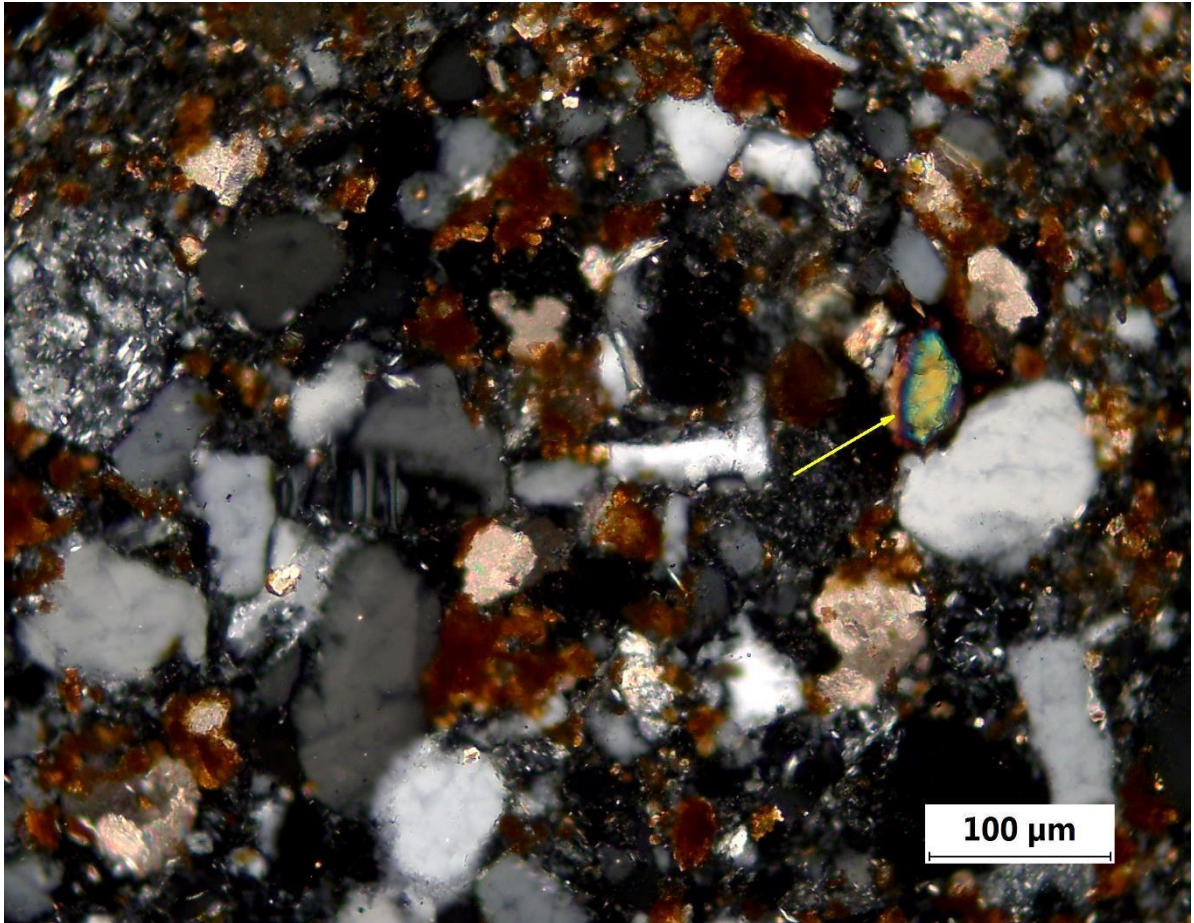


Figure 2.13. Thin section photomicrograph of facies 3 from location 1. This image shows a birefringent tourmaline grain (yellow arrows), poor sorting, quartz grains, feldspar grains and angular to sub-angular crystals. Photograph with crossed polarizers.

Mineralogy

In location 1, 16 samples were analyzed for mineralogy, 14 samples from location 2, and 3 samples from location 3. Column 8 of the sections in figures 2.13-2.15 show locations where samples were taken. The feldspar category contains both K-feldspar and plagioclase (Tables 2.2-2.4). Some minerals identified were categorized as “Other minerals” (Tables 2.2-2.4), and include: nacrite, bytownite, phlogopite, magnesium iron aluminum silicate, ferrihydrite, pyrochroite, iron oxide, chalcopyrite, gypsum, phengite, goethite, anatase, and titanium oxide.

Tables 2.2-2.4 do not include the mineralogy of individual A-bed and B- beds, the mineralogy of these specific bed types is presented in Figures 2.16-2.18 and in Tables 3.4-3.6. Dolomite is the dominant mineral in facies 1 with small amounts of quartz, feldspar, and kaolinite. In facies 2, dominant minerals are quartz and feldspars, with minor muscovite and kaolinite while in facies 3 the dominant minerals are quartz and feldspars with muscovite, illite, and kaolinite.

Table 2.2. XRD mineralogy from location 1. Feldspar minerals include; albite (AL), microcline (MC), and orthoclase (ORTH). Mica and clay minerals include: biotite (BT), muscovite (MS), kaolinite (KL) and illite (IL). Sixteen samples were analyzed. Numbers in the columns are the weight percentages.

Sample	Quartz	Feldspar	Mica & Clay	Calcite	Dolomite	Others
D13-89A	12	1 (AL 1)	3 (BT 1, KL 2)	0	83	1
D13-89B	7	1 (AL 1)	1 (KL 1)	0	91	0
F14-07C	14	2 (AL 2)	2 (KL 2)	0	78	4
F14-07E	35	19 (AL 4, MC 15)	10 (KL 4, MS 6)	0	21	15
D13-89C	6	4 (AL 1, MC 3)	5 (BT 4, KL 1)	0	85	0
D13-89D	26	10 (AL 4, MC 6)	24 (KL 4, MS 20)	0	18	22
D13-89E	12	5 (AL 2, ORTH 3)	6 (KL 3, MS 3)	0	71	6
D13-89F	9	6 (AL 4, ORTH 2)	17 (KL 12, MS 5)	0	55	13
D13-89G	25	2 (AL 2)	17 (KL 17)	0	55	1
F14-08D	47	0	24 (KL 24)	0	21	8
D13-89H	29	17 (MC 17)	22 (KL 21)	5	27	0
F14-09D	45	29 (MC 29)	26 (KL15,MS 11)	0	0	0
F14-09F	22	10 (MC 10)	65 (KL39, MS 26)	0	0	3
F14-09I	45	16 (MC 16)	35 (IL 23, KL 12)	0	0	4
F14-09J	21	50 (MC 50)	28 (IL 9, KL 19)	0	0	1
D13-89I	30	46 (AL 6, MC 40)	23 (IL 8, KL 15)	0	0	1

Table 2.3. XRD mineralogy from location 2. Feldspar minerals include; albite (AL), microcline (MC), and orthoclase (ORTH). Mica and clay minerals include: biotite (BT), muscovite (MS), kaolinite (KL) and illite (IL). Fourteen samples were analyzed. Numbers in the columns are the weight percentages.

Sample	Quartz	Feldspar	Mica & Clay	Calcite	Dolomite	Others
F14-12O	7	2 (AL 2)	1 (KL 1)	0	90	0
F14-12A	15	30 (AL 19, SN 11)	0	1	38	16
F14-12B	20	13 (AL 9, MC 4)	64 (KL 15, MS49)	0	3	0
F14-12C	1	12 (AL 7, MC 5)	7 (IL5, KL 2)	0	80	0
F14-12D	2	23 (AL 5, MC 18)	12 (IL 9, KL 3)	0	63	0
F14-12E	2	23 (AL 14, MC 9)	10 (IL 8, KL 2)	0	65	0
F14-12F	17	43 (AL 24, MC19)	6 (IL 4, KL 2)	0	34	0
F14-12G	32	41 (AL 27, MC14)	25 (IL 18, KL 7)	0	2	0
F14-12H	27	27 (AL 11, MC16)	32 (KL 24, MS 8)	0	14	0
F14-12I	17	21 (AL 9, MC 12)	29 (KL 16, MS13)	0	32	1
F14-12J	20	30 (AL 14, MC16)	34 (KL 20, MS14)	0	10	6
F14-12K	19	31 (AL 9, MC 22)	29 (KL 17, MS12)	0	15	6
F14-12L	23	36 (AL 20, MC16)	28 (KL 15, MS13)	0	8	5
F14-12M	20	35 (AL 17, MC 18)	39 (KL 23, MS 16)	0	0	6

Table 2.4. XRD mineralogy from location 3. Feldspar minerals include; albite (AL), microcline (MC), and orthoclase (ORTH). Mica and clay minerals include: biotite (BT), muscovite (MS), kaolinite (KL) and illite (IL). Three samples were analyzed. Numbers in the columns are the weight percentages.

Sample	Quartz	Feldspar	Mica & Clay	Calcite	Dolomite	Others
F14-18K	18	0	5 (KL, 5)	0	57	20
F14-18L	20	6 (MC 6)	36 (KL 8, MS 28)	0	38	0
F14-18M	35	0	41 (KL 9, MS 32)	0	21	3

Sections

Three sections were measured in the northern Kingston Range area, one from each location. The sections are about 4 meters thick and include the Beck Spring – Kingston Peak contact. Both field and laboratory data are presented with the graphical representation of the sections including: grain size trends, lithologies, sedimentary structures, contacts, XRD mineralogy, SEM-EDS chemical composition, and facies designations. Typical trends in the data include a generally up-section increase in clastics, decrease in dolomite and increase in grain size (Figures 2.13-2.15).

Sedimentary structures are few and they include: alternating thick laminae and thin beds, sub parallel laminations, lenticular structures, and faint ripple cross bedding. At the base of KP₁, dolostone is interbedded with siltstone/mudstone and fine sand. Detailed study of this interbedded unit is presented later in this study.

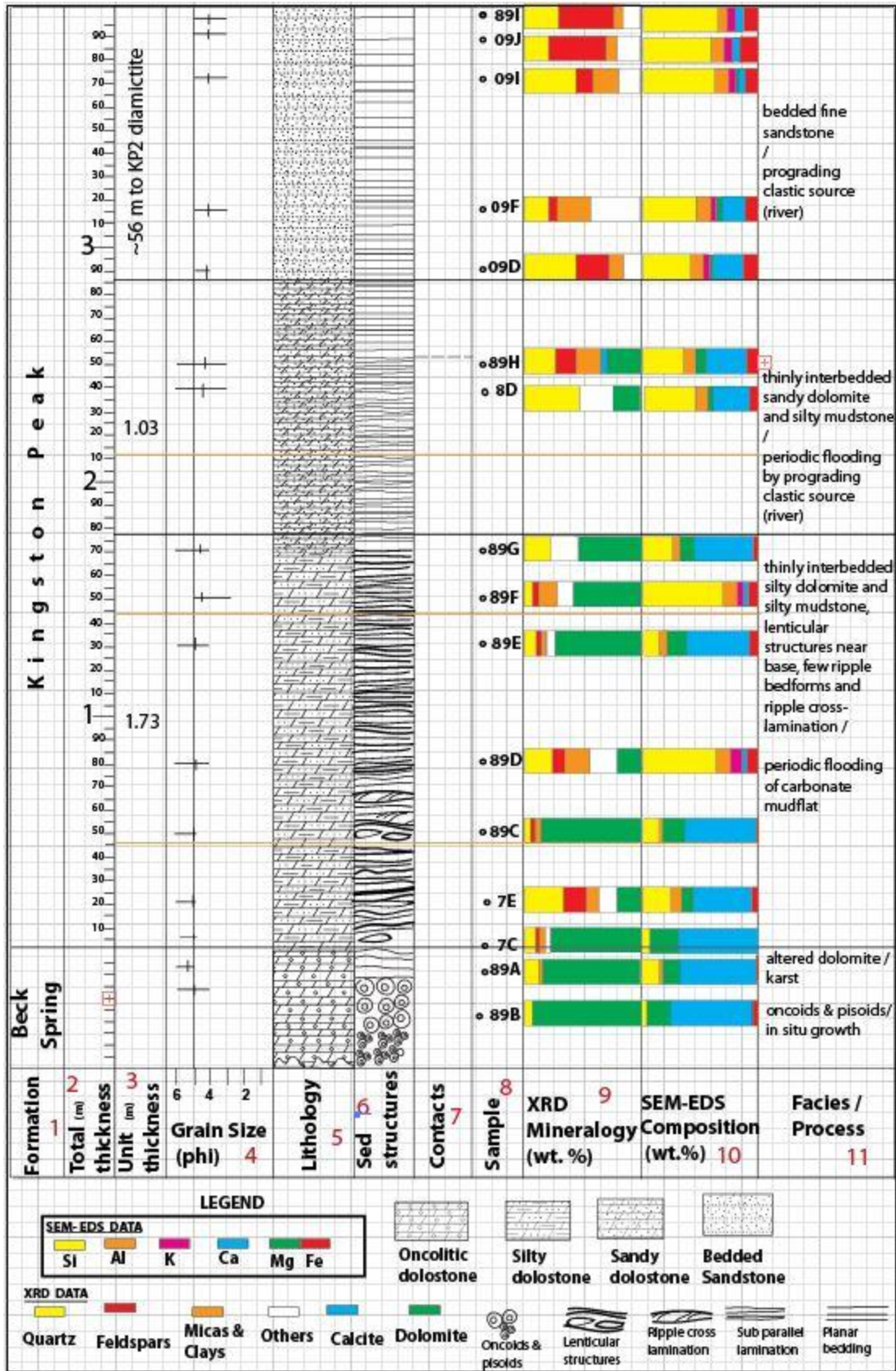


Figure 2.14. Section 1. Names of the formations measured are shown on the first column. Column two and three show total and unit thicknesses in meters. Trends in grain size are supported by measurements in the lab. The fifth, sixth and seventh column show lithologies, sedimentary structures, and contacts. Sample locations are shown by dots. Column nine shows mineral percentages in the sample. Column ten shows chemical percentages in the sample. Column eleven shows facies that were named

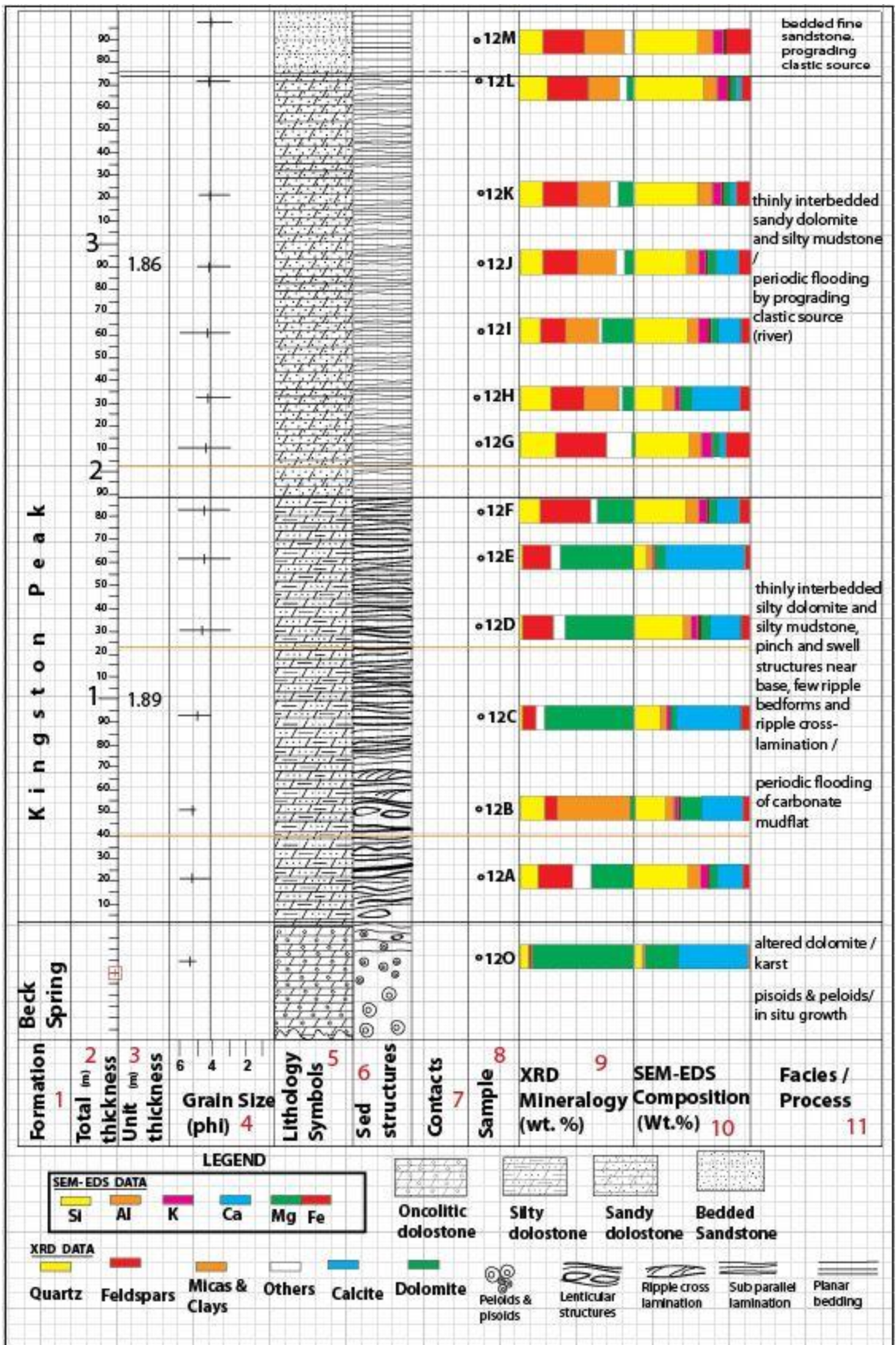


Figure 2.15. Section 2. Names of the formations measured are shown on the first column. Column two and three show total and unit thickness in meters. Trends in grain size are supported by measurements in the lab. The fifth, sixth and seventh column show lithologies, sedimentary structures and contacts. Sample locations are shown by dots. Column nine shows mineral percentages in the sample. Column ten shows chemical percentages in the sample. Column eleven shows facies that were identified.

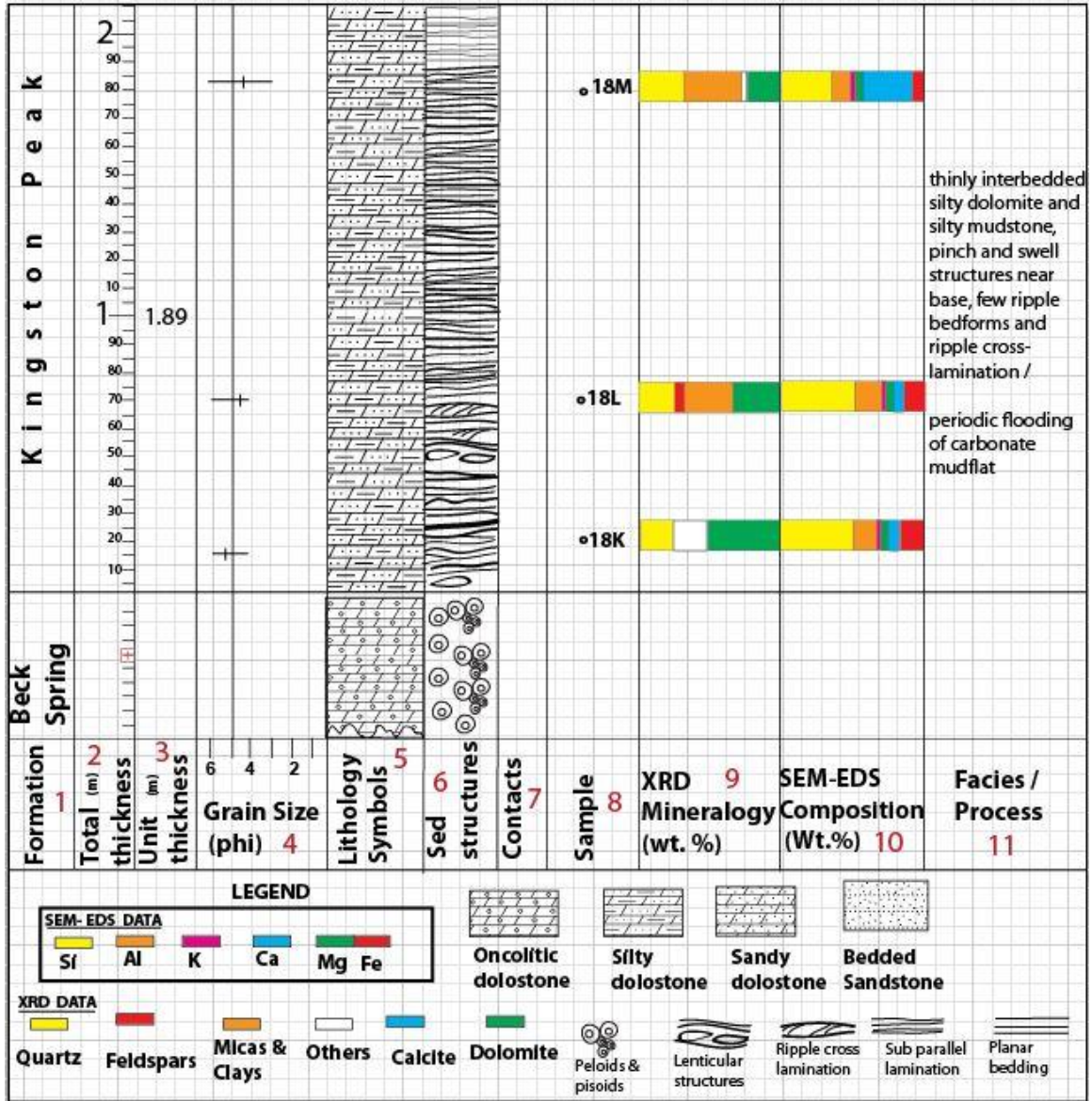


Figure 2.16. Section 3. Names of the formations measured are shown on the first column. Column two and three show total and unit thickness in meters. Trends in grain size are supported by measurements in the lab. The fifth, sixth and seventh column show lithologies, sedimentary structures and contacts. Sample locations are shown by dots. Column nine shows mineral percentages in the sample. Column ten shows chemical percentages in the sample. Column eleven shows facies that were identified.

A and B Beds

These are the alternating clastic--rich and dolomite-rich thin beds identified and described in all three locations studied. The clastic rich beds are generally dolomitic, silty to sandy mudstone and the dolomite rich beds are generally silty dolostones. In this study, clastic rich thin beds were named A-beds and dolomite rich thin beds were named B-beds.

These alternating beds are found at the base of KP₁ and they don't occur in the Beck Spring Dolomite. In all three locations studied, five samples, each with A and B thin beds, were taken for chemical and mineralogical analysis (Tables 3.4-3.6 & 3.10-3.12). The results are presented in Figures 2.16- 2.18.

Typical trends in the data are that A-beds have more quartz, feldspars, mica and clay with less dolomite. B-beds have more dolomite and few clastic grains. In a few cases there is no dolomite at all in A-beds, but all B-beds have some small amounts of clastic materials.

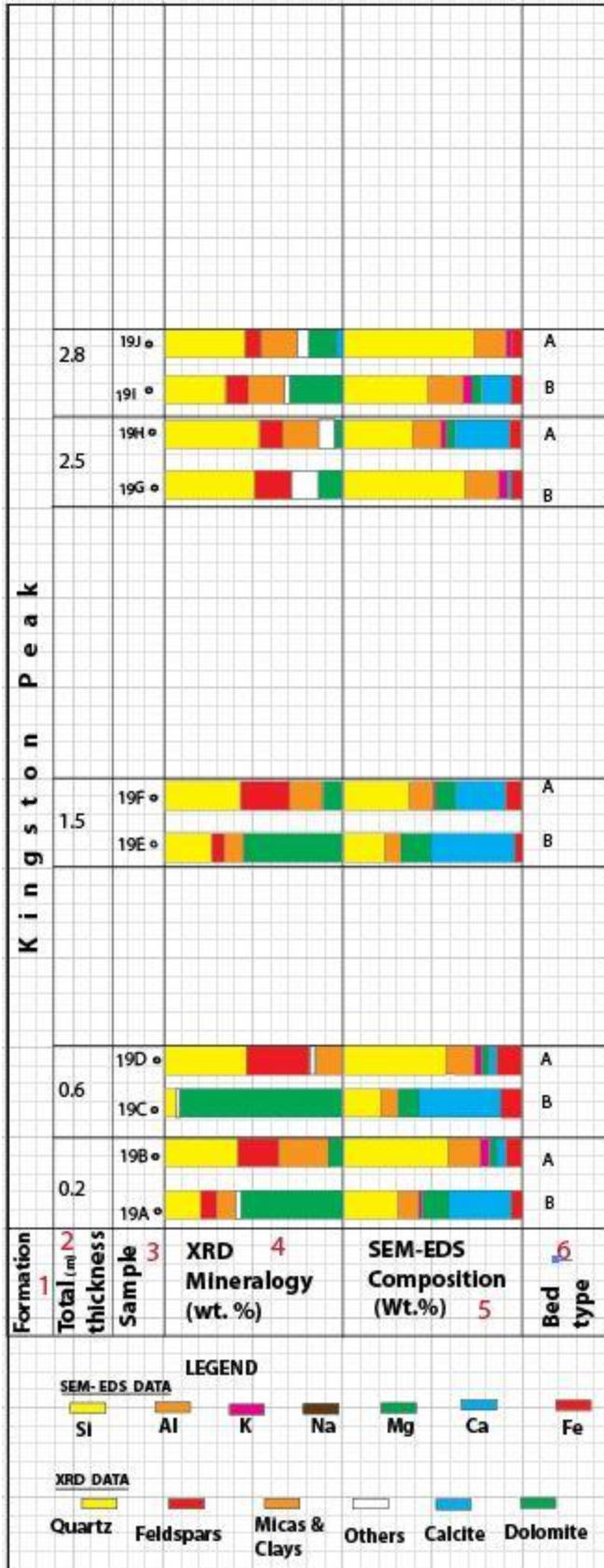


Figure 2.17. Detailed section of the base of section measured at location 1. Section shows details of analysis from facies 2 thin alternating beds. Names of the Formation measured are shown on the first column. Column two shows total thickness in meters. Sample locations are shown by dots in column three. Trends in mineralogy are shown in in column four. Chemical trends are shown in column five. Column six represents bed type

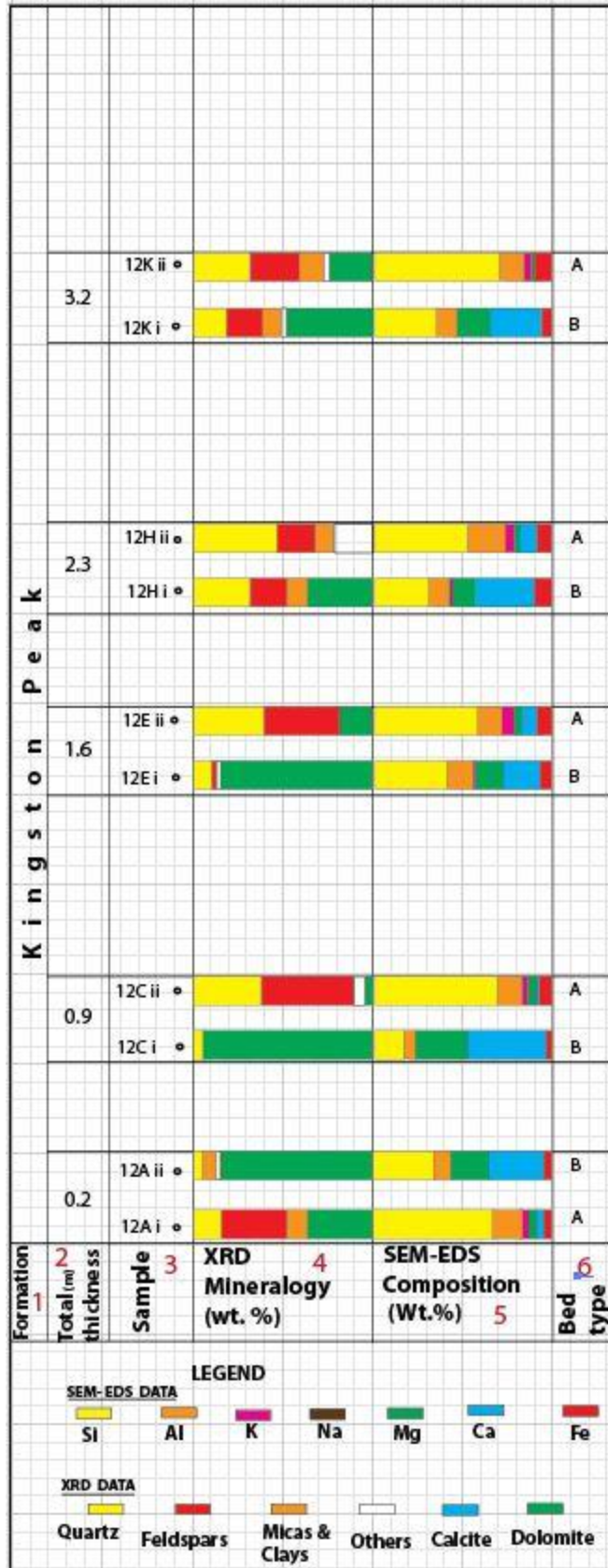


Figure 2.18. Detailed section of the base of section measured at location 2. Section shows details of analysis from facies 2 thin alternating beds. Names of the Formation measured are shown on the first column. Column two shows total thickness in meters. Sample locations are shown by dots in column three. Trends in mineralogy are shown in in column four. Chemical trends are shown in column five. Column six represents bed type.

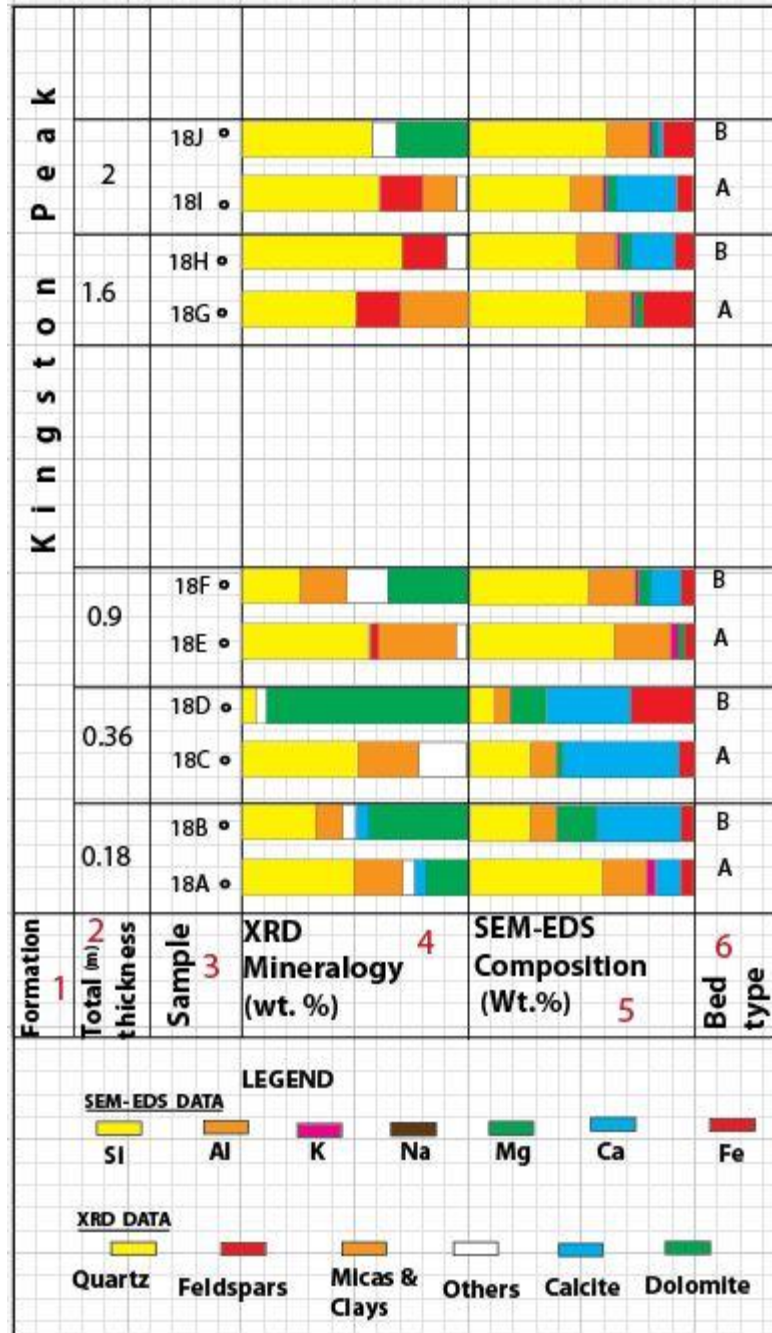


Figure 2.19: Detailed section of the base of section measured at location 3. On facing page. Section shows details of analysis from facies 2 thin alternating beds. Names of the Formation measured are shown on the first column. Column two shows total thickness in meters. Sample locations are shown by dots in column three. Trends in mineralogy are shown in in column four. Chemical trends are shown in column five. Column six represents bed type.

Bed Thickness in Facies 2

The top of the Beck Spring Dolomite shows a dramatic change at the contact with Kingston Peak Formation (Figures 2.2- 2.4). At the base of Kingston Peak Formation are alternating thin A and B beds. At location 1, the alternating thin beds unit (facies 2) is about 2.5 meters thick. In location 2 it is about 3.7 meters thick while in location 3 it is about 2 meters thick. The alternating thin beds were measured individually in all 3 sections and their measurements recorded in Tables 3.13-3.15.

The alternating thin beds show a rapid increase in bed thickness from millimeter scale to meter scale thickly bedded sandstone. Using measurements from the individual beds, average thickness trends were graphed by plotting bed number against the net cumulative thickness. This graph illustrates relative accumulation trends that can be correlated among the three locations studied (Figure 2.20).

The graph in Figure 2.20 is of cumulative bed thickness with an equal subsidence value subtracted from each bed at each location and addition of an equal stretch factor for each bed for each location. The subsidence values used are: 16mm/bed for location 1 and 12 mm/bed for location 2 and 3. Stretch factors are: 1.1 for location 1, 1.0 for location 2, and 1.5 for location 3.

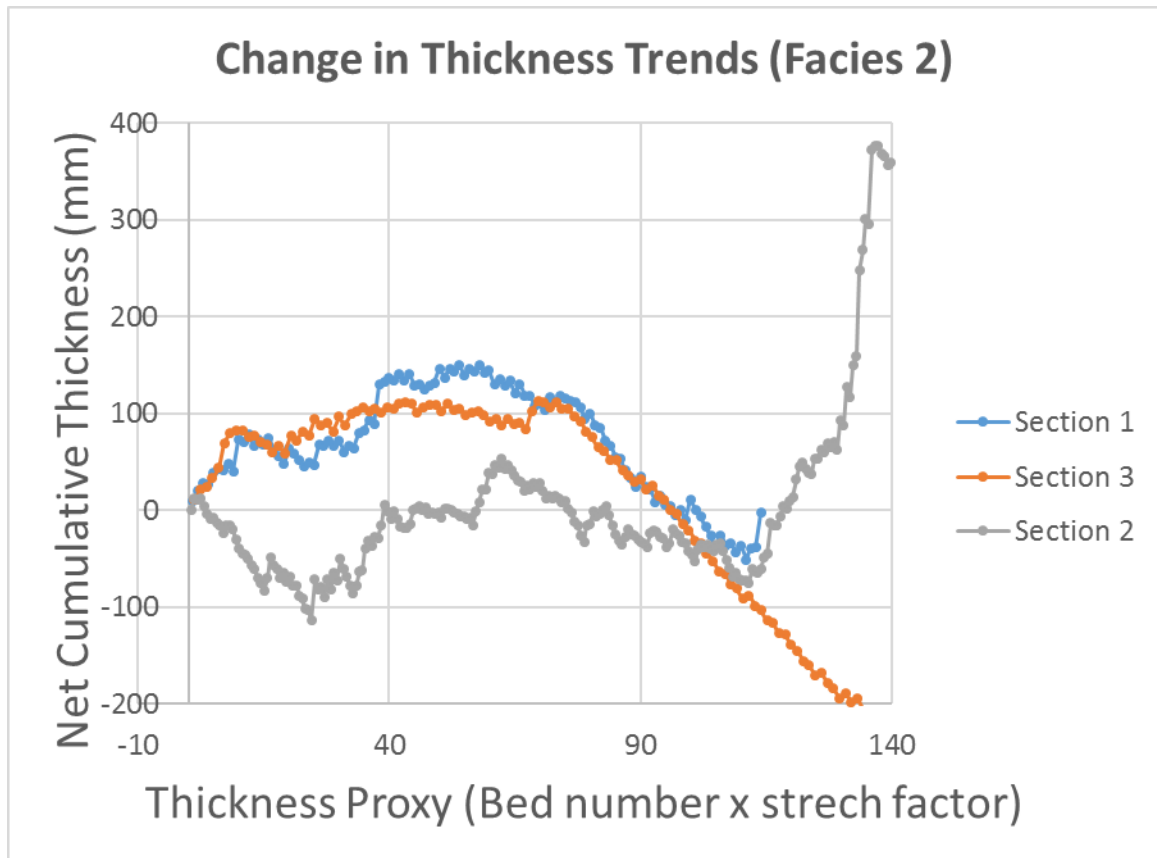


Figure 2.20: Graph of relative accumulation trends for the thin beds measured in the three locations of this study. Trends correlate among sections. These trends are partly independent of lithology. Stretch factors are: 1.1 for location 1, 1.0 for location 2, and 1.5 for location 3.

Discussion

Provenance

Interpreting the provenance of sedimentary rocks is a major goal in sedimentology. Nowadays provenance has a wider scope than just an interpretation of source area. It also involves deciphering distance to the source area, lithology of source area, tectonic setting of source area together with climate and relief (Boggs, 2009).

Sedimentary provenance aims at interpreting the sediment's history through its entire detrital spectrum from initial erosion from the parent rocks to its final burial stage (Weltje and von Eynatten, 2004). To achieve this aim, compositional and textural properties of sediments are analyzed. Comprehensive and meaningful provenance interpretation demands that we recognize and appreciate factors other than composition of source rocks that can affect final composition. Source rock composition is the first order control on sediment composition, other controls include climate and relief, sediment transport, depositional environment and diagenesis (Boggs, 2009; Bridge and Demicco, 2008; Weltje and von Eynatten, 2004).

Most studies of sedimentary provenance employ petrographic analysis of quartz, feldspars, micas, accessory minerals and rock fragments as provenance indicators (Scholle et al., 2014). One or more of these indicators may be missing in particular sedimentary rocks under study. The fact that one or more indicators may be missing does not imply that they were not in the source rock, it means that we recognize that provenance studies are complicated and hence need for caution in our conclusions. We can only use provenance indicators that are present in the rocks being studied (Boggs, 2009). In this study, quartz, feldspars, and accessory minerals have been examined as the available indicators of provenance.

Provenance from Quartz

Quartz characteristics that have been examined in previous studies for possible provenance signature include: inclusions, undulatory extinction, polycrystallinity and

crystal shape (Boggs, 2009; Scholle et al., 2014). In this study, extinction, polycrystallinity and crystal shape properties have been used.

Most thin sections examined in this study show the majority of quartz grains exhibit unit or non-undulatory extinction with few crystals exhibiting undulatory extinction. Most quartz grains are single crystals with very few polycrystals. Crystal shapes range from angular to sub angular and they are not elongated.

In first cycle rocks, highly undulatory extinction has been suggested to be diagnostic of a metamorphic source rocks while non-undulatory extinction is diagnostic of igneous source rocks. Polycrystalline quartz has been suggested to be most indicative of metamorphic rocks (Boggs, 2009). Another study suggests that unit extinction to slightly undulatory extinction indicate a plutonic or metamorphic source, however a metamorphic one will have some elongated grains (Scholle et al., 2014).

Poor sorting, abundant feldspars, angular to sub-angular quartz crystals and abundant matrix suggest that the rocks in this study are first cycle deposits. Unit extinctions to slightly undulatory extinctions of quartz crystals in this study together with extremely rare quartz polycrystals and a lack of elongated crystal shapes suggest a plutonic origin of quartz.

Provenance from Feldspars

Feldspars are useful minerals in interpreting source rocks as they are chemically and mechanically less stable than quartz, hence less likely to be recycled, although some may be recycled under some conditions. Their reliability can be seriously hampered by

weathering, transport, and diagenesis hence detrital feldspar composition does not necessarily reflect composition of source rocks (Boggs, 2009).

Feldspar provenance indicators are in most cases based on their mineralogy, zoning, twinning, and chemical composition (Boggs, 2009; Bridge and Demicco, 2008; Scholle et al., 2014). In this study, feldspars mineralogy has been used.

Feldspars mineralogy provides crude provenance information due to the fact that they can be derived from more than one kind of igneous or metamorphic rocks (Boggs, 2009). Potassium /alkali feldspars are constituents of felsic igneous, pegmatites, and intermediate metamorphic sources. The feldspars common in plutonic and high grade metamorphic rocks are orthoclase and microcline while sanidine and anorthoclase are common in volcanic rocks (Boggs, 2009; Scholle et al., 2014).

Plagioclase feldspars are particularly common in volcanic rocks; however, they may also occur in some plutonic igneous and metamorphic sources. Plagioclase feldspars unfortunately are easily albitized during diagenesis thus reducing compositional information that can be traced to source rocks (Boggs, 2009).

In this study, abundant microcline suggests plutonic source more than a volcanic one. Furthermore, microcline is common in some plutonic sources. Abundant microcline and a significant percentage of albite can also suggest a metamorphic origin, but this is unlikely because feldspar grains are not elongated. Accounting for all observations in facies 2 and 3 rocks, feldspar mineralogy suggests a plutonic igneous source.

Provenance from Accessory Minerals

Accessory minerals are major indicators of provenance although many are subject to alteration through chemical and mechanical processes (Boggs, 2006; Boggs, 2009; Bridge and Demicco, 2008; Scholle et al., 2014). Use of entire accessory mineral assemblages and use of single mineral groups are two main approaches that have been used to obtain provenance information from accessory minerals (Boggs, 2009; Scholle et al., 2014). In this study, the entire accessory mineral assemblage approach has been used although it was based on thin section observations rather than mineral separates.

The approach of using an entire accessory mineral assemblage has two main assumptions that hinder its effectiveness in provenance interpretation. The first assumption is that each major kind of source rock yields a distinctive assemblage of accessory minerals. The second assumption states that the accessory mineral assemblages that occur in the detrital sediments accurately reflect what was in the parent rock (Boggs, 2009).

In this study, only three relevant accessory minerals have been identified through XRD analysis and thin section examinations, they include muscovite, biotite and tourmaline. The percentage of biotite is so small that it is not recognizable in the thin section. Muscovite is abundant and clearly seen both in XRD analysis and in thin sections. One possible explanation for this case could be due to the fact that muscovite is more stable than biotite. It is likely therefore that most biotite crystals were destroyed through chemical and mechanical processes. The presence of few biotite, abundant muscovite grains and tourmaline suggest an acidic igneous parent.

Provenance from Textural Immaturity

Poor sorting, abundant feldspars, angular to sub-angular crystals, abundant matrix, and rock fragments are major indicators of sediment immaturity (Bridge and Demicco, 2008). In this study, general poor sorting, abundant feldspars, angular to sub-angular crystal shapes, and abundant matrix in the form of clays and clay-size feldspar and quartz, strongly suggest that the sediments are immature and first cycle.

Immature sediments in this study suggest a minimal amount of chemical weathering which according to Bridge and Demicco (2008) could mean two major possibilities. One, mainly physical weathering occurred at high altitude or a slope. Two, a likelihood of a rapid transport, deposition and burial. It is possible that the immature sediments in this study are associated with the rifting during the Neoproterozoic time period.

Paleoenvironmental Interpretation of Facies

Facies 1: Altered Dolostones

Beck Spring Dolomite has been interpreted as an assemblage deposited in a shallow marine carbonate environment (Corsetti et al., 2003; Marian and Osborne, 1992). Proterozoic carbonate tidalites consist of microbialites and other carbonates grains suggesting carbonate production by chemical and microbial processes (Davis and Dalrymple, 2012). Although skeletal metazoans are not found prior to Cambrian, Precambrian carbonates appear to have been deposited in environmental settings surprisingly similar to those of the Phanerozoic (Davis and Dalrymple, 2012).

Most fossil oncoids occur in peritidal settings in shallow environments (Tucker and Wright, 1990). Pisoids and ooids can form in a wide range of environments although

the majority of them in the geological record formed in very shallow marine settings. However, pisoids and ooids themselves alone are not diagnostic of any specific environment (Tucker and Wright, 1990).

Peloids are key components of shallow marine carbonates although interpreting their exact origin is very difficult (Tucker and Wright, 1990). Microbial laminations are sedimentary structures produced by episodic deposition of microbial mats that help to trap sediments that then grow to re-establish themselves on a new sediment surface (Bridge and Demicco, 2008). However, such laminae cannot always be associated with microbial mats because non-organic processes can produce such laminae. For example, wavy laminae described in this study can be formed by wave ripples and crinkled ones can result from soft sediment deformation (Bridge and Demicco, 2008). Laminated mudstones and sandstones widely interpreted as microbial are common in shallow water carbonates (Bridge and Demicco, 2008).

Most carbonate sediment is generated in the shallow subtidal zone and then carried to other tidal zones by storms, waves, and tidal currents (Tucker and Wright, 1990). Subtidal carbonate sediments generally contain oncoids, peloids, microbialites, and many other carbonate grains (Davis and Dalrymple, 2012). In this study, the presence of oncoids, pisoids, peloids and microbial laminations in facies 1 suggest that it was probably deposited on a shallow marine carbonate setting in a subtidal zone.

Facies 2: Interbedded Dolostones and Silty Mudstones

This facies can be described as a mixed carbonate-siliciclastic facies. Some deposits within the Beck Spring Dolomite south of Central Saddle Peak Hills contain

mixed carbonate-siliciclastic beds but differ from the ones described in this study. They have been interpreted as fluvial-tidal deposits (Marian and Osborne, 1992). The thin alternating carbonate-siliciclastic beds found in this facies have also been described as transition beds by some researchers (Corsetti and Kaufman, 2003; Macdonald et al., 2013).

The thin alternating beds in this study seem to have been formed under tidal influence. Like other sedimentary structures formed under tidal influence, these also seem to reflect flood, slack and ebb condition of tidal cycles (Davis and Dalrymple, 2012). During flood and ebb periods of a tidal cycle, relatively coarse sediments are deposited and during high and low slack, fine suspended sediments settles to the bottom resulting in an alternation of coarse and fine materials in thin beds that are sometimes called tidal bedding (Davis and Dalrymple, 2012). Tidal bedding units tend to be only millimeter to centimeters thick and they are in most cases heterolithic although some can be monolithic (Davis and Dalrymple, 2012). The thin alternating beds in this study which can be described as tidal heterolithic bedding can occur most likely in two tidal environments; tide dominated delta and tidal flats.

Tide Dominated Delta

Tide dominated deltas are the primary regressive coastal environment at the mouths of rivers that prograde due to the input of sediments by rivers resulting in an upward coarsening succession (James and Dalrymple, 2010). Tide dominated deposits tend to be heterolithic, especially deposits immediately seaward of active distributaries (Davis and Dalrymple, 2012; James and Dalrymple, 2010). In tide dominated deltas, tidal

currents are dominant and wave currents usually subordinate (Bridge and Demicco, 2008).

Thin beds of sand-mud cycles are common in tide dominated deltas and they are products of flood-slack-ebb-slack tidal currents (Davis and Dalrymple, 2012). Thin beds in most cases occur where sediment supply is high enough to permit at least a millimeter of deposition in every twelve hours and this condition is best satisfied along margins of channels, delta front and prodeltaic settings (James and Dalrymple, 2010). High suspended loads are likely to produce lenticular bedding; however lenticular bedding can occur by processes other than tidal currents and to infer a tidal influence requires cyclicity (James and Dalrymple, 2010). It is possible that the alternating thin beds described in this study are of tidal origin and specifically of a tide dominated delta.

Tidal Flats.

A common feature of tidal flats is the shoreward fining in grain size resulting in upward fining successions (Boggs, 2006). However, a coarsening upward succession can occur in a tidal flat. Deposition from tidal currents that are decelerating in time as well as in space in a tidal flat setting will give rise to fining upward succession and deposition from tidal currents that are decelerating in space but accelerating in time will generate a coarsening upward succession (Boggs, 2009; Bridge and Demicco, 2008). This study exhibits coarsening upward successions.

In areas where ripples are formed by maximum tidal currents, ripples cease to move during slackening periods and drapes of mud settle from the suspension. Repetition of this process gives rise to heterolithic bedding which can be described as flaser, wavy

and lenticular (Bridge and Demicco, 2008). This type of heterolithic bedding is common in tidal flats; however basic alternation of sand and mud can occur in any environment where there is periodic variation in current strength. Cyclicity can be a key to invoking tidal origin (Bridge and Demicco, 2008; James and Dalrymple, 2010). Mixed sand and mud is more common in the middle intertidal zone of the tidal flat (Boggs, 2006). As outlined above, it is possible to explain the structures of the alternating thin beds in this study as heterolithic lenticular beds formed by tidal currents in tidal flat setting.

Mixed Carbonate- Siliciclastic Deposits

Mixed carbonate- siliciclastic facies are common in both ancient and modern deposits (Mount, 1984). Processes which can cause this mixing have been grouped into four categories: (A) punctuated mixing, where extreme periodic events transfer sediments from one depositional environment to another; (B) facies mixing, where sediments are mixed along the diffuse boundaries between contrasting facies; (C) in situ mixing, where the carbonate fraction consists of the autochthonous or parautochthonous death assemblages of calcareous organisms that accumulated on or within siliciclastic substrates(this may not apply in the Precambrian); and (D) source mixing, where admixtures are formed by the uplift and erosion of nearby carbonate source terranes (Mount, 1984).

The mixed carbonate- siliciclastic deposits of facies 2 in this study are most likely the product of punctuated mixing where tidal currents probably transported carbonate sediments from facies 1(subtidal) and siliciclastic sediments from facies 3(clastic source).

However, it is unknown whether the Proterozoic and Phanerozoic mixing took place in the same ways and in the same environments (Mount, 1984).

Facies 3: Bedded Fine Sandstones

These fine sandstones lack clear sedimentary structures that can help in paleoenvironmental interpretation. However, one possible explanation as to how these massive beds of sandstones were deposited above thin, alternating fine-grained beds is that they were deposited when the river inflow extended into a relatively deep marine waters where the flow was detached from the bed and therefore was unable to move the bedload beyond the detachment point. Turbulent mixing was probably intense near the river mouth and much of the coarser suspended and the bedload was deposited as the fine grained sediments were transported farther before deposition to be part of thin alternating bed (Boggs, 2006).

Correlations

There are similar oncoids and pisoids in the Beck Spring Dolomite in all three locations studied. Mineralogy and mineral trends are similar in the three locations studied and they can be correlated. Generally, in each location, dolomite is the dominant mineral in facies 1 with small amounts of quartz, feldspar, and kaolinite. In facies 2, dominant minerals are quartz and feldspars, with minor muscovite and kaolinite while in facies 3 the dominant minerals are quartz and feldspars with muscovite, illite, and kaolinite (Tables 2.2-2.4).

Similar thicknesses of facies 2 can be correlated: in location 1, it is about 2.5 meters thick, in location 2 it is about 3.7 meters thick, and in location 3 it is about 2

meters thick. At all three locations, the first diamictites of the Kingston Peak Formation appear about 60 meters above the BSD-KPF contact. The thin alternating beds in facies 2 that were measured individually in all three locations and their measurements recorded in Tables 3.13-3.15, were graphed and they generated relative accumulation trends that can be correlated among the three locations studied (Figure 2.20).

Beck Spring Dolomite - Kingston Peak Formation Boundary

Researchers in the Pahrump Group have defined BSD-KPF boundary using lithology change (Macdonald et al., 2013; Miller, 1985; Mrofka, 2010; Prave, 1999). In this study BSD-KPF boundary is defined by an abrupt change in lithology. Depending on the locality, the contact between BSD and KPF in the Panamint Range has been described as conformable, inter-fingering and unconformable (Miller, 1985).

In the Eastern side of the Death Valley, the BSD-KPF contact has been described as gradational by some workers (Macdonald et al., 2013; Prave, 1999). In the Alexander Hills and Saratoga Hills, the BSD-KPF contact has been described as transitional and in the southern Black Mountains it has been described as sharp contact (Mrofka and Kennedy, 2011).

In this study there is an abrupt change in lithology from dolostones to clastics (Figures 2.3-2.5). This abrupt change in lithology on the boundary between BSD and KPF can be described as a sharp contact. The BSD-KPF contact at Kingston Range in this study most likely represent a sequence boundary as evidenced by a change in lithology from dolostones to clastics.

Conclusions

The contact between Beck Spring Dolomite and Kingston Peak Formation is covered over most outcrops in the Kingston Range. Only three exposures were found with the contact. The BSD-KPF contact at Kingston Range most likely represent a sequence boundary as evidenced by a change in lithology from dolostones to clastics.

This study has successfully correlated three sections within the northern Kingston Range. The correlation is possible due to similar sedimentary features, mineralogy, processes, bed thickness, and distance between the first diamictite bed in the Kingston Peak Formation and the contact with the Beck Spring Dolomite.

All three outcrops have a unit consisting of alternating thin beds which in this study are named A (clastic rich) and B (dolomite rich). Three facies have been identified in the sedimentary succession studied with one facies having subfacies. The presence of oncoids, pisoids, peloids and microbial laminations in facies 1 suggest that it was probably deposited on a shallow marine carbonate setting in a subtidal zone. The thin alternating beds in facies 2 which look like tidal heterolithic bedding seem to have been formed under tidal influence in two possible tidal environments; tide dominated delta and tidal flats. The pattern of increasing clastic grains and increasing clastic bed thickness upsection suggest clastic influx during progradation that progressively overwhelmed carbonate production. This progradational setting could have occurred on a tide dominated delta or on a prograding tidal flat.

Poor sorting, angular to sub-angular grains shapes, abundant matrix, and abundant feldspars in the clastic sediments indicate that the sediments are immature. The immature sediments are likely to be similar to that of source rock (Bridge and Demicco, 2008). Petrographic analysis of quartz extinction and polycrystalline characteristics, feldspars

mineralogy and accessory minerals in this study suggest an igneous source and most likely acidic igneous origin. These observations are for a small part of the Kingston Range where the contact of the Kingston Peak Formation with the Beck Spring Dolomite has been found.

References

- Boggs, S., 2006, Principles of Sedimentology and Stratigraphy, 4th edn, USA, Pearson Prentice Hall.
- Boggs, S., 2009, Petrology of Sedimentary Rocks, 2nd edn, USA, Cambridge University Press.
- Bridge, J., and Demicco, R., 2008, Earth surface processes, landforms and sediment deposit, USA, Cambridge university Press.
- Corsetti, F. A., and J. Kaufman, A., 2003, Stratigraphic investigations of carbon isotope anomalies and Neoproterozoic ice ages in Death Valley, California: Geological Society of America Bulletin, v. 115, no. 8, p. 916-932.
- Davis, R. A., and Dalrymple, R. W., 2012, Principles of Tidal Sedimentology, USA, Springer Publishers.
- Fedo, C. M., and Cooper, J. D., 2001, Sedimentology and sequence stratigraphy of Neoproterozoic and Cambrian units across a craton-margin hinge zone, southeastern California, and implications for the early evolution of the Cordilleran margin: Sedimentary Geology, v. 141, p. 501-522.
- Gutstadt, A. M., 1968, Petrology and depositional environments of the Beck Spring dolomite (Precambrian), Kingston Range, California: Journal of sedimentary petrology, v. 38, no. 4, p. 1280-1289.
- Hewett, D. F., 1940, New formation names to be used in the Kingston Range, Ivanpah quadrangle, California: Washington Academy of Sciences, v. 30, no. 6, p. 239-240.
- James, N. P., and Dalrymple, R. W., 2010, Facies Model 4, Canada, Geological Association of Canada.
- Labotka, T. C., Albee, A. L., Lanphere, M. A., and McDowell, S. D., 1980, Stratigraphy, structure, and metamorphism in the central Panamint Mountains (Telescope Peak quadrangle), Death Valley area, California: Summary: Geological Society of America Bulletin, v. 91, no. 3, p. 125.
- Loyd, S. J. s., and Corsetti, F. A., 2010, The origin of the millimeter-scale lamination in the Neoproterozoic lower Beck Spring Dolomite: Implications for widespread, fine scale, layer-parallel diagenesis in Precambrian carbonates: Journal of Sedimentary Research, v. 80, no. 7-8, p. 678-687.
- Macdonald, F. A., Prave, A. R., Petterson, R., Smith, E. F., Pruss, S. B., Oates, K., Waechter, F., Trotzok, D., and Fallick, A. E., 2013, The Laurentian record of

Neoproterozoic glaciation, tectonism, and eukaryotic evolution in Death Valley, California: *Geological Society of America Bulletin*, v. 125, no. 7-8, p. 1203-1223.

- Mahon, R. C., 2012, Detrital Zircon Provenance, Geochronology and Revised Stratigraphy of the Mesoproterozoic and Neoproterozoic Pahrump (Super) Group, Death Valley Region, California and Geology of the Saddle Peak Hills 7.5' Quadrangle, San Bernardino County, California [M.S. thesis]: Idaho State University.
- Mahon, R. C., Dehler, C. M., Link, P. K., Karlstrom, K. E., and Gehrels, G. E., 2014, Geochronologic and stratigraphic constraints on the Mesoproterozoic and Neoproterozoic Pahrump Group, Death Valley, California: A record of the assembly, stability, and breakup of Rodinia: *Geological Society of America Bulletin*.
- Marian, M. L., and Osborne, R. H., 1992, Petrology, petrochemistry, and stromatolites of the Middle to Late Proterozoic Beck Spring Dolomite, eastern Mojave Desert, California: *Canadian Journal of Earth Sciences*, v. 29, p. 2595-2609.
- Miller, J. M. G., 1985, Glacial and syntectonic sedimentation: The upper Proterozoic Kingston Peak Formation, southern Panamint Range, eastern California: *Geological Society of America Bulletin*, v. 96, no. 12, p. 1537.
- Miller, J. M. G., 1987, Paleotectonic and stratigraphic implications of the Kingston Peak-Noonday contact in the Panamint Range, eastern California: *Journal of Geology*, v. 95, no. 1, p. 75-85.
- Mount, J. F., 1984, Mixing of siliciclastic and carbonate sediments in shallow shelf environments: *Geology*, v. 12, p. 432-435.
- Mrofka, D., and Kennedy, M., 2011, The Kingston Peak Formation in the eastern Death Valley region :The Geological Record of Neoproterozoic Glaciations: *Geological Society Memoir*, no. 36, p. 449-458.
- Mrofka, D. D., 2010, Competing Models for the Timing of Cryogenian Glaciation: Evidence from the Kingston Peak Formation, Southeastern California [Ph.D. thesis]: Riverside, California, University of California at Riverside.
- Petterson, R., 2009, Glacigenic and related strata of the Neoproterozoic Kingston Peak Formation in the Panamint Range, Death Valley region, California. II. The basal Ediacaran Noonday Formation, eastern California, and implications for Laurentian equivalents. III. Rifting of southwest Laurentia during the Sturtian–Marinoan interglacial: The Argenta Orogeny [Ph.D. thesis]: California Institute of Technology.

- Prave, A. R., 1999, Two diamictites, two cap carbonates, two delta C-13 excursions, two rifts: The Neoproterozoic Kingston Peak Formation, Death Valley, California: *Geology*, v. 27, no. 4, p. 339-342.
- Scholle, D. S. U., Scholle, P. A., Schieber, J., and Raine, R. J., 2014, A color guide to the petrography of sandstones, siltstones, shale and associated rocks, USA, *American Association of Petroleum Geologist*, v. 109.
- Stewart, J. H., 1972, Initial Deposits in the Cordilleran Geosyncline: Evidence of a Late Precambrian (<850 m.y.) Continental Separation: *Geological Society of America Bulletin*, v. 83, no. 5, p. 1345.
- Tucker, M. E., 1986, Formerly aragonitic limestone associated with tillites in the Late Proterozoic of Death Valley, California: *Journal of Sedimentary Petrology*, v. 56, no. 6, p. 818-830.
- Tucker, M. E., and Wright, V. P., 1990, *Carbonate Sedimentology, USA*, Blackwell Publishing.
- Walker, J. D., Klepacki, D. W., and Burchfiel, B. C., 1986, Late Precambrian tectonism in the Kingston Range, southern California: *Geology*, v. 14, no. 1, p. 15.
- Weltje, G. J., and von Eynatten, H., 2004, Quantitative provenance analysis of sediments: review and outlook: *Sedimentary Geology*, v. 171, no. 1-4, p. 1-11.

CHAPTER THREE

EXPANDED CONCLUSIONS AND FUTURE RESEARCH

In this study, we have made significant contributions to the study of the upper Beck Spring Dolomite and lower Kingston Peak Formation especially on the Eastern side of the Death Valley and specifically in the Beck Canyon area, Kingston Range. These include correlation of the thin alternating beds and a detailed sedimentological study of outcrops with an abrupt change from Beck Spring Dolomite to Kingston Peak Formation at a higher resolution. This study has shed some light about the sedimentology of the Beck Spring-Kingston Peak transition. However, there are several additional questions that need to be resolved.

Observations, interpretations, and conclusions in this study are from the northern Kingston Range. Although this has produced excellent results for this area, other areas with possible Beck Spring-Kingston Peak contacts have not been studied in detail. The same study in other areas within the Pahrump Group may reveal additional conclusions.

Similar studies in other Neoproterozoic sedimentary basins around the world can help in a better understanding of environmental transitions during the Neoproterozoic time period. In future, I intend to carry out a similar study in the Neoproterozoic sedimentary basins of Namibia in Africa.

APPENDIX A

X-RAY DIFFRACTION DATA FROM KINGSTON RANGE LOCATIONS

Table 3.1. XRD data for location 1 in weight percentages.

SAMPLE	QUARTZ	FELDSPAR	MICA & CLAYS	CALCITE	DOLOMITE	OTHERS
D13-89A	12	1	3	0	83	1
D13-89B	8	1	1	0	91	0
F14-07C	14	2	2	0	78	4
F14-07E	35	19	10	0	21	15
D13-89C	6	4	5	0	85	0
D13-89D	26	10	24	0	18	22
D13-89E	12	5	6	0	71	7
D13-89F	9	6	17	0	55	13
D13-89G	25	2	17	0	55	18
F14-08D	47	0	24	0	21	32
D13-89H	29	17	23	5	27	2
F14-09D	45	29	26	0	0	15
F14-09F	22	10	65	0	0	42
F14-09I	45	16	35	0	0	17
F14-09J	21	50	28	0	0	20
D13-89I	31	48	23	0	0	16

Table 3.2. XRD data for location 2 in weight percentages.

SAMPLE	QUARTZ	FELDSPAR	MICA & CLAYS	CALCITE	DOLOMITE	OTHERS
F14-12O	7	2	1	0	90	0
F14-12A	15	30	0	1	38	16
F14-12B	21	13	64	0	3	0
F14-12C	1	12	7	0	80	7
F14-12D	2	23	12	0	63	12
F14-12E	2	23	10	0	65	10
F14-12F	17	43	6	0	34	6
F14-12G	32	41	25	0	2	25
F14-12H	27	27	31	0	14	4
F14-12I	17	22	29	0	32	2
F14-12J	20	30	35	0	10	8
F14-12K	19	31	30	0	16	7
F14-12L	23	36	28	0	8	6
F14-12M	20	34	39	0	0	8

Table 3.3. XRD data for location 3 in weight percentages.

SAMPLE	QUARTZ	FELDSPAR	MICA& CLAY	CALCITE	DOLOMITE	OTHERS
F14-18K	18	0	5	0	57	24
F14-18L	20	6	36	0	39	0
F14-18M	35	0	41	0	21	4

APPENDIX B

Table 3.4. XRD data for location 1 A and B thin beds in weight percentages.

SAMPLE	QUARTZ	FELDSPAR	MICA&CLAYS	CALCITE	DOLOMITE	OTHERS
F14-19A	21	7	10	0	59	3
F14-19B	42	22	28	0	8	0
F14-19C	9	0	0	0	89	2
F14-19D	48	33	14	0	0	4
F14-19E	27	10	7	0	54	0
F14-19F	44	26	18	0	12	0
F14-19G	52	19	0	0	14	16
F14-19H	52	13	22	0	4	8
F14-19I	36	13	19	0	29	3
F14-19J	45	9	20	3	15	7

Table 3.5. XRD data for location 2 A and B thin beds in weight percentages.

SAMPLE	QUARTZ	FELDSPAR	MICA&CLAY S	CALCITE	DOLOMITE	OTHER S
F14-12Ai	16	36	14	0	35	0
F14-12Aii	6	0	8	0	83	4
F14-12Ci	7	0	0	0	93	0
F14-12Cii	40	51	0	0	5	5
F14-12Ei	12	4	0	0	79	5
F14-12Eii	40	43	0	0	18	0
F14-12Hi	33	20	12	0	36	0
F14-12Hii	49	20	11	0	0	21
F14-12Ki	18	23	10	0	46	3
F14-12Kii	36	27	13	0	24	0

Table 3.6. XRD data for location 3 A and B thin beds in weight percentages.

SAMPLE	QUARTZ	FELDSPAR	MICA&CLAYS	CALCITE	DOLOMIT E	OTHERS
F14-18A	50	0	20	4	20	6
F14-18B	35	0	13	5	42	5
F14-18C	52	0	26	0	0	22
F14-18D	9	0	0	0	85	6
F14-18E	55	5	3	0	0	7
F14-18F	27	0	22	3	35	13
F14-18G	52	18	30	0	0	0
F14-18H	70	20	0	0	0	10
F14-18I	62	18	15	0	0	5
F14-18J	58	0	0	0	32	10

APPENDIX C

SEM-EDS from Kingston Range locations.

Table 3.7. SEM-EDS data for location 1 in weight percentages.

Sample	NaO	MgO	Al ₂ O ₃	SiO ₂	CaO	Fe ₂ O ₃	K ₂ O
D13-89A	0	25	3	15	54	2	0
D13-89B	0	23	1	6	65	5	0
F14-07C	0	29	1	11	57	2	0
F14-07E	0	15	10	30	38	4	2
D13-89C	0	25	4	17	52	2	0
D13-89D	0	3	16	68	2	5	5
D13-89E	0	22	9	18	44	5	1
D13-89F	0	2	16	72	2	6	3
D13-89G	0	17	9	29	39	4	1
F14-08D	0	7	12	52	18	6	3
D13-89H	0	10	13	43	26	5	2
F14-09D	0	5	12	51	19	9	3
F14-09F	0	8	12	54	15	8	3
F14-09I	0	3	14	68	4	7	4
F14-09J	0	3	15	64	5	9	4
Di3-89I	1	2	13	71	4	6	4

Table 3.8. SEM-EDS data for location 2 in weight percentages.

Sample	NaO	MgO	Al ₂ O ₃	SiO ₂	CaO	Fe ₂ O ₃	K ₂ O
F14-12O	0	35	2	10	52	1	0
F14-12A	2	8	12	54	15	5	4
F14-12B	2	21	10	31	30	4	1
F14-12C	1	6	9	27	50	6	2
F14-12D	2	10	10	51	20	5	3
F14-12E	1	10	5	15	64	4	1
F14-12F	2	9	11	52	15	7	3
F14-12G	1	6	16	55	2	15	5
F14-12H	0	12	14	32	34	7	2
F14-12I	2	8	11	54	15	6	4
F14-12J	2	9	12	52	15	7	3
F14-12K	2	5	15	62	4	9	4
F14-12L	2	5	14	66	2	6	4
F14-12M	0	7	15	49	17	6	4

Table 3.9. SEM-EDS data for location 3 in weight percentages.

Sample	NaO	MgO	Al ₂ O ₃	SiO ₂	CaO	Fe ₂ O ₃	K ₂ O
F14-18K	0	3	16	53	9	15	3
F14-18L	0	4	17	59	7	11	3
F14-18M	0	6	14	37	32	9	3

APPENDIX D

Table 3.10. SEM-EDS data for location 1 A and B thin beds in weight percentages.

Sample	NaO	MgO	Al ₂ O ₃	SiO ₂	CaO	Fe ₂ O ₃	K ₂ O
F14-19A	0	15	12	31	33	7	2
F14-19B	1	6	17	60	5	8	4
F14-19C	0	13	10	21	42	13	1
F14-19D	1	6	15	54	5	14	4
F14-19E	0	18	9	24	42	4	1
F14-19F	0	11	13	37	26	10	3
F14-19G	0	1	17	63	3	8	5
F14-19H	0	4	15	45	26	6	3
F14-19I	0	7	15	48	17	6	4
F14-19J	0	2	17	68	2	4	4

Table 3.11. SEM-EDS data for location 2 A and B thin beds in weight percentages.

Sample	NaO	MgO	Al ₂ O ₃	SiO ₂	CaO	Fe ₂ O ₃	K ₂ O
F14-12Ai	1	5	12	67	5	4	5
F14-12Aii	1	17	9	35	32	4	2
F14-12Ci	0	29	4	16	47	3	1
F14-12Cii	1	4	13	70	2	6	5
F14-12Ei	1	13	13	42	17	9	2
F14-12Eii	2	5	11	59	11	8	8
F14-12Hi	0	10	12	31	31	12	2
F14-12Hii	0	4	19	53	9	9	5
F14-12Ki	1	17	9	36	29	6	2
F14-12Kii	2	4	13	69	2	6	5

Table 3.12. SEM-EDS data for location 3 A and B thin beds in weight percentages.

Sample	NaO	MgO	Al ₂ O ₃	SiO ₂	CaO	Fe ₂ O ₃	K ₂ O
F14-18A	0	2	19	59	7	5	4
F14-18B	0	18	10	26	38	5	1
F14-18C	0	3	9	26	51	8	1
F14-18D	0	15	8	13	37	26	1
F14-18E	1	3	19	65	2	5	5
F14-18F	0	5	19	53	12	8	3
F14-18G	1	4	16	50	2	22	3
F14-18H	0	7	18	47	15	11	3
F14-18I	1	6	13	45	26	7	2
F14-18J	0	2	18	62	3	10	4

APPENDIX E

A & B bed thickness data from Kingston Range locations

Table 3.13 A and B bed thickness data for location 1 in millimeters. BN-Bed Number.
BT- Bed Thickness

BN	BT	BN	BT	BN	BT	BN	BT	BN	BT	BN	BT	BN	BT
1a	10	10a	7	19a	11	28a	5	37a	10	46a	5	55a	7
1b	24	10b	29	19b	51	28b	21	37b	20	46b	12	55b	20
2a	22	11a	10	20a	17	29a	12	38a	13	47a	3	56a	2
2b	13	11b	9	20b	19	29b	21	38b	11	47b	20	56b	25
3a	26	12a	8	21a	12	30a	7	39a	14	48a	6	57a	15
3b	17	12b	14	21b	20	30b	16	39b	10	48b	14	57b	47
4a	14	13a	12	22a	9	31a	2	40a	3	49a	6		
4b	21	13b	33	22b	20	31b	19	40b	20	49b	19		
5a	7	14a	14	23a	4	32a	9	41a	3	50a	5		
5b	44	14b	19	23b	16	32b	19	41b	13	50b	34		
6a	12	15a	10	24a	9	33a	3	42a	2	51a	5		
6b	22	15b	19	24b	19	33b	23	42b	10	51b	8		
7a	4	16a	4	25a	17	34a	4	43a	3	52a	5		
7b	21	16b	20	25b	28	34b	14	43b	14	52b	6		
8a	9	17a	13	26a	6	35a	5	44a	4	53a	4		
8b	21	17b	28	26b	23	35b	17	44b	7	53b	26		
9a	3	18a	18	27a	12	36a	8	45a	6	54a	5		
9b	9	18b	24	27b	20	36b	27	45b	24	54b	16		

Table 3.14. A and B bed thickness data for location 2 in millimeters. BN-Bed Number.
BT- Bed Thickness.

BN	BT	BN	B T	BN	BT	BN	BT	BN	BT	BN	BT	BN	BT
1a	0	10a	8	19a	1	28a	13	37a	14	46a	26	55a	18
1b	25	10b	6	19b	11	28b	35	37b	9	46b	22	55b	8
2a	10	11a	7	20a	1	29a	20	38a	14	47a	25	56a	16
2b	14	11b	3	20b	55	29b	6	38b	5	47b	12	56b	4
3a	4	12a	7	21a	2	30a	22	39a	14	48a	21	57a	5
3b	4	12b	4	21b	14	30b	11	39b	11	48b	10	57b	14
4a	6	13a	25	22a	2	31a	25	40a	13	49a	22	58a	9
4b	14	13b	34	22b	30	31b	33	40b	7	49b	9	58b	15
5a	6	14a	3	23a	1	32a	5	41a	21	50a	22	59a	9
5b	9	14b	9	23b	30	32b	4	41b	12	50b	1	59b	8
6a	5	15a	2	24a	4	33a	20	42a	11	51a	16	60a	14
6b	20	15b	18	24b	34	33b	4	42b	9	51b	6	60b	4
7a	11	16a	2	25a	2	34a	4	43a	10	52a	7	61a	8
7b	8	16b	17	25b	3	34b	11	43b	10	52b	7	61b	3
8	2	17a	3	26a	3	35a	12	44a	12	53a	10	62a	7
8b	3	17b	13	26b	4	35b	16	44b	9	53b	3	62b	2
9a	6	18a	1	27a	20	36a	27	45a	14	54a	18	63a	5
9b	11	18b	9	27b	27	36b	13	45b	4	54b	8	63b	30
64a	13	73a	8	82a	9	91a	16	100a	12	109a	15	118a	10
64b	25	73b	27	82b	15	91b	24	100b	21	109b	12	118b	13
65a	7	74a	14	83a	8	92a	15	101a	9	110a	5	119a	30
65b	14	74b	11	83b	9	92b	44	101b	21	110b	9	119b	11
66a	16	75a	7	84a	19	93a	9	102a	8	111a	2	120a	35
66b	17	75b	10	84b	13	93b	12	102b	18	111b	15	120b	30
67a	2	76a	3	85a	4	94a	22	103a	4	112a	7	121a	7
67b	1	76b	16	85b	3	94b	22	103b	42	112b	9	121b	14
68a	3	77a	26	86a	4	95a	10	104a	7	113a	20	122a	8
68b	6	77b	9	86b	3	95b	20	104b	51	113b	39	122b	72
69a	8	78a	9	87a	15	96a	16	105a	2	114a	24	123a	15
69b	20	78b	5	87b	6	96b	30	105b	45	114b	26	123b	85
70a	19	79a	11	88a	11	97a	25	106a	22	115a	22	124a	27
70b	8	79b	4	88b	12	97b	16	106b	100	115b	45	124b	70
71a	10	80a	8	89a	9	98a	6	107a	33	116a	16		
71b	8	80b	5	89b	26	98b	8	107b	44	116b	40		
72a	10	81a	25	90a	10	99a	11	108a	7	117a	15		
72b	10	81b	17	90b	11	99b	28	108b	89	117b	20		

Table 3.15. A and B bed thickness data for location 3 in millimeters. BN-Bed Number.
BT- Bed Thickness.

BN	BT	BN	BT	BN	BT	BN	BT	BN	BT
1a	11	13a	18	25a	5	37a	5	49a	6
1b	15	13b	2	25b	4	37b	3	49b	1
2a	10	14a	16	26a	10	38a	10	50a	7
2b	14	14b	10	26b	3	38b	1	50b	1
3a	15	15a	11	27a	13	39a	11	51a	4
3b	25	15b	5	27b	4	39b	1	51b	1
4a	15	16a	10	28a	9	40a	5	52a	5
4b	10	16b	5	28b	4	40b	1	52b	1
5a	8	17a	12	29a	20	41a	5	53a	10
5b	3	17b	7	29b	15	41b	1	53b	1
6a	9	18a	11	30a	7	42a	4	54a	4
6b	4	18b	9	30b	5	42b	1	54b	1
7a	6	19a	7	31a	11	43a	6	55a	12
7b	3	19b	2	31b	4	43b	1	55b	2
8a	12	20a	12	32a	8	44a	3	56a	10
8b	3	20b	9	32b	2	44b	1	56b	1
9a	20	21a	8	33a	5	45a	6	57a	7
9b	5	21b	4	33b	1	45b	1	57b	1
10a	14	22a	13	34a	4	46a	5	58a	4
10b	5	22b	4	34b	1	46b	1	58b	1
11a	20	23a	9	35a	6	47a	10	59a	5
11b	3	23b	3	35b	1	47b	1	59b	1
12a	10	24a	10	36a	8	48a	5		
12b	2	24b	9	36b	1	48b	1		